Permeability and its effect on the utilization of geothermal energy

Tapio Envall

Master's Thesis
University of Jyväskylä
Department of Physics
20.08.2008

Abstract

Geothermal energy is a clean and renewable source of energy. Although its contribution to world's energy production is minor at present, new techniques, especially the promising Hot Dry Rock method (HDR), have potential to make geothermal energy a significant form of energy. HDR power plants require neither areas of volcanic activity nor natural geothermal fluids, and they can be built almost anywhere in the world. Despite the vast energy potential HDR method can provide, drilling techniques, measurement systems, modelling problems, long-term effects, relative uncontrollability and lack of knowledge of the reservoir's behaviour pose a continuous challenges for HDR development.

One of the key parameters controlling the amount of flow and productivity of a HDR plant is the permeability of the reservoir. Thus it is crucial to be able to estimate and increase the permeability. As an example of permeability measurement, permeabilities of 21 rock samples were determined by measuring flow of helium gas through the samples. In addition, by using the known porosities of the samples, the product of specific area and tortuosity was determined by Carman-Kozeny equation. Also, the relations of structural and transport parameters were reviewed.

Preface

The work reported in this Master's thesis has been done between June 2006 and January 2008 at the Department of Physics in the University of Jyväskylä. The purpose of this thesis was to review the geothermal energy and promising HDR method with a special focus on the effect of permeability. In addition, permeability measurements of the rock samples from Kaali meteor crater were included to this thesis.

I would like to thank my supervisors Prof. Jussi Timonen and Dr. Jussi Maunuksela, who have been excellent advisors both in the theoretical field and in helping the writing process of this Master's thesis. In addition, I thank Ph.D. student Mikko Voutilainen for familiarizing me with the measuring equipment. Finally, I wish to thank my friends Veikko, Niko and Lauri for sharing my anguish during the writing process.

Jyväskylä 20th August, 2008

Tapio Envall

Contents

Chapter 1

Introduction

The world's need for clean, renewable sources of energy is obvious. A form of renewable energy is the geothermal energy that is the heat energy inside the Earth. In places which are not naturally suitable for straigth-forward geothermal applications, but still have enough heat deep in the rocks of the earth, the geothermal system for a plant can be partly constructed artificially. This procedure, called HDR for "Hot Dry Rocks" is significant because of the vast heat potential it can utilize.

Heat extraction procedure requires heat transfer from hot rocks into the circulating fluid. The amount of flow through the rock is determined by the permeability of the bedrock, and it is thus a crucial parameter for the plant's performance. Therefore, matters affecting and ways to increase the permeability of the rock are reviewed. In addition, the operations from construction to running of an HDR plant are discussed.

As an example of the ways the crucial transport parameter, permeability, can be determined, the permeabilities of 21 rock samples from Kaali meteor crater, Saaremaa, Estonia were measured. Motivation for these measurements has come from Tartu University, where the effect of meteor impact on the properties of the rock matrix is studied. Total of 41 rock samples have been sent to Jyväskylä University. The permeability was reasonably measurable for 21 of these samples. Thus this thesis completes the work of Ph.D. student Mikko Voutilainen, who measured the porosities of all samples in his master's thesis [1]. The final analysis for these rock samples is carried out by Tartu University.

The equipment used for these measurements is based on the permeation of helium gas through rock sample. After helium has permeated through the sample, it can be

detected by a mass spectrometer calibrated for helium. Helium is small and inert gas and thus it diffuses through the rock samples relatively fast and without harming them.

Chapter 2

Permeability

In order to define permeability of the medium, it has to be porous. By porous medium we mean a material consisting of a solid matrix with an interconnected void. The porosity ε of the material is defined as the volume fraction of the void - the volume of voids divided by the total volume of the medium (solid matrix and void space). Thus the porosity is a dimensionless quantity and its value lies between 0 and 1. [2, 3]

2.1 Darcy's law

Permeability (specific/intrinsic) is a physical quantity that characterizes the amount of fluid that permeates through it in the presence of pressure difference. The contribution of properties of the fluid (e.g. viscosity) and of the mechanism of permeation are excluded from this definition of permeability. Thus it is a purely geometrical parameter, uniquely determined by the pore structure. [4]

The permeability k is defined by Darcy's law. In sufficiently slow, unidirectional, steady flow the volume flow Q [m^3/s], of the fluid through the sample is given by

$$Q = -\left(\frac{kA}{\mu}\right)\left(\frac{\Delta p}{L}\right), \tag{2.1}$$

or in the differential form

$$Q = -\left(\frac{kA}{\mu}\right)\left(\frac{dp}{dL}\right), \tag{2.2}$$

where A is the normal cross-sectional area of the sample [m^2], L is the length of the sample [m], μ is the (dynamic) viscosity of the fluid (for helium $\mu = 2,0 \cdot 10^{-5} \frac{Ns}{m^2}$ at T = 300 K [5]) and Δp is the pressure difference across the ends of the sample [Pa].[1]

Often the porous media are anisotropic in their nature, resulting in direction dependence of permeability. Thus, exact characterization of flow phenomena should be presented with the aid of tensors. Generally in three dimensions, permeability $\mathbb{K}$ is a second-order tensor, and Darcy's law generalizes to

$$\mathbf{v} = -\frac{1}{\mu}\mathbb{K} \cdot \nabla p, \tag{2.3}$$

where $\mathbf{v}$ is the so-called Darcy velocity of the fluid, meaning the average velocity of the fluid, taken over summed volume of both the medium and the fluid [2].[2]

Theoretical backing for Darcy's law has been obtained with the help of various types of models, and results of Darcy's law have been confirmed by countless measurements. The SI-unit for permeability is m^2, but sometimes the unit of *Darcy*, which equals $0,987 \cdot 10^{-12}$ m^2, is used.

If the fluid is gas (as it is in the measurements of this thesis), the above mentioned forms of Darcy's law are unable to describe the permeation. Due to compressibility of gases, the volume flow Q depends on the pressure and thus the mere pressure difference is insufficient to characterize the motion of the gas.

At first, the fluid flow is assumed to be at steady state, meaning that the mass is not accumulated in the medium and thus the mass flow at every point of the sample is assumed constant. Let subscript 1 indicate the side of the sample from where the gas enters (injection side), and 2 the outlet side (flushing side). Quantities at an arbitrarily chosen point of the sample are denoted by symbols without subscripts. Thus the mass flow through the sample is

[1] Strictly speaking, p appearing in the equation above is so called piezometric pressure, defined as $p = P + \rho g z$, where P is the hydraulic pressure, ρ the density of the fluid, g is the accelaration due to gravity and z is the distance measured vertically upward from an arbitrarily chosen datum level. But as the fluid used in this thesis was helium gas, the effect of this gravity term is neglible by all practical means.

[2] In one-dimensional case with uniform cross-sectional area, $\mathbf{v} = \frac{Q}{A}$, as noted in eqs (2.1) and (2.2).

$$\begin{aligned}
& \dot{m}_1 = \dot{m} = \dot{m}_2 \\
\iff \quad & \rho_1 \dot{V}_1 = \rho \dot{V} = \rho_2 \dot{V}_2 \\
\iff \quad & \rho_1 A_1 v_1 = \rho A v = \rho_2 A_2 v_2 \qquad | : A_1 = A = A_2 \\
\iff \quad & \rho_1 v_1 = \rho v = \rho_2 v_2, \qquad (2.4)
\end{aligned}$$

where $\dot{m}$ is the mass flow [kg/s], ρ is the density of the gas [kg/m^3], $\dot{V}$ is the volume flow [m^3/s] (volume flow at the flushing side was earlier noted by $Q := \dot{V}_2$) and A is the normal cross-sectional area of the sample [m^2], which is assumed to be constant at every point of the sample, from which the last equality follows.

On the other hand, considering the gas as an ideal gas, its density can be expressed in the form

$$\rho = \frac{pM}{RT}, \qquad (2.5)$$

where p is the pressure, M the molecular mass of the gas, R the universal gas constant and T the temperature [6]. Thus

$$\begin{aligned}
pv &= \frac{RT}{M}\frac{pM}{RT}v = \frac{RT}{M}\rho v \\
&= \frac{RT}{M}\rho_2 v_2 = \frac{RT}{M}\frac{p_2 M}{RT}v_2 \\
&= p_2 v_2, \qquad (2.6)
\end{aligned}$$

where eqs (2.4) and (2.5) are used and the temperature profile is assumed constant. By rearranging the differential form of Darcy's law (eqn (2.2)), we find

$$v\ dL = \frac{Q}{A}\ dL = -\frac{k}{\mu}\ dp$$

and by multiplying this by p we further find that

$$pv\ dL = -\frac{k}{\mu} p\ dp.$$

Inserting the result eqn (2.6) into this equation results in

$$p_2 v_2\ dL = -\frac{k}{\mu} p\ dp.$$

Integrating this result over sample length yields

$$\begin{aligned}
\int_0^L p_2 v_2 \, dL &= \int_{p_1}^{p_2} -\frac{k}{\mu} p \, dp \\
\iff \qquad p_2 v_2 \int_0^L dL &= -\frac{k}{\mu} \int_{p_1}^{p_2} p \, dp \\
\iff \qquad p_2 v_2 L &= -\frac{k}{\mu} \frac{1}{2} (p_2^2 - p_1^2) \\
\iff \qquad p_2 \frac{Q}{A} L &= -\frac{k}{\mu} \frac{1}{2} (p_2^2 - p_1^2) \\
\iff \qquad Q &= -k \frac{A}{\mu L} \frac{p_2^2 - p_1^2}{2 p_2}, \qquad (2.7)
\end{aligned}$$

where Q is the volume flow at the outlet of the sample. This is the appropriate form of Darcy's law for compressible (ideal) gases at steady state with constant temperature.

Plotting measurement points, such that the x-component equals the pressure term $A(p_2^2 - p_1^2)/(2\mu L p_2)$ and the y-component the volume flow Q, one gets a family of points of linear orientation. After linear regression to such data, slope of the linear fit equals the permeability of the sample according to eqn (2.7). Theoretically, fitting a line through only one of such measurement point and the origin would yield a value for permeability according to Darcy's law. However, typically permeability measurements involve relatively high experimental errors, and thus it is highly advisable to use many data points for the linear fit.

2.2 Carman-Kozeny equation

There is no universal relationship between porosity and permeability. However, with the aid of specific area and tortuosity such relation (called Carman-Kozeny equation) can be expressed. First we assume that cross-sectional area of the medium is constant. The channel diameter D_h controlling the flow is assumed to be four times the hydraulic radius, which is defined as the void volume of the medium V_S divided by the surface

area of channels in medium (A_{FS})

$$\begin{aligned} D_h &= \frac{4 \cdot \text{ void volume}}{\text{surface area}} \\ &= \frac{4\varepsilon \cdot V}{A_{FS}} \\ &= \frac{4\varepsilon \cdot V_S}{A_{FS} \cdot (1-\epsilon)} \\ &= \frac{4\varepsilon}{\frac{A_{FS}}{V_S}(1-\varepsilon)} \\ &= \frac{4\varepsilon}{A_0(1-\varepsilon)}, \end{aligned} \tag{2.8}$$

where $V_S = (1-\epsilon)V$ is the solid volume of the medium and $A_0 = A_{FS}/V_S$ is the specific area (or volumetric area).

The pore velocity v_p and the filter velocity v (in Darcy's law) are related by equation $v_p = v\frac{\tau}{\varepsilon}$ [4], where τ is the tortuosity of the medium, defined as the actual length of the flowpath divided by the shortest distance across the sample. Inserting this into Darcy's law (eqn (2.1)) we find

$$\begin{aligned} v_p &= \frac{k\tau}{\mu\varepsilon}\nabla p \\ &= \frac{1}{D_H^2} D_H^2 \frac{k\tau}{\mu\varepsilon}\nabla p \\ &= \frac{A_0^2(1-\varepsilon)^2}{16\varepsilon^2} D_H^2 \frac{k\tau}{\mu\varepsilon}\nabla p, \end{aligned} \tag{2.9}$$

where the last equality follows from eqn (2.8). This may be rewritten as

$$v_p = \frac{1}{k_0\tau}\frac{D_H^2}{16\mu}\nabla p, \tag{2.10}$$

where shape parameter $k_0 = \frac{\varepsilon^3}{A_0^2(1-\varepsilon^2)k\tau^2}$ [3].[3]

Thus,

$$k = \frac{\varepsilon^3}{A_0^2(1-\varepsilon)^2 k_0 \tau^2,} \tag{2.11}$$

[3]The choice of k_0 originates from so-called Hagen-Poiseuille equation for laminar flow of cylinder of uniform cross-sectional area, given as $v_{max} = -\frac{D^2}{16\mu}\nabla p$ [7], which is of the same form as eqn (2.10), scaled with shape parameter and tortuosity.

which is called *Carman-Kozeny equation for permeability*. Theory and experiments verify that the shape parameter k_0 is fairly constant. Theories state that it is 2 for circular capillary and lies within 2,0 and 2,5 for rectangular, elliptical and annular shapes [3], and measurements confirm that values of k_0 seem to lie between 2,0 and 3,0 [4]. Thus, often the approximation $k_0 \approx 2,5$ is made. If we know porosity and permeability of the sample, the product $A_0\tau$ can be estimated by this approximation,

$$A_0\tau = \sqrt{\frac{\varepsilon^3}{2,5(1-\varepsilon)^2 k}}. \tag{2.12}$$

In a geothermal context the so-called flow impedance Z is often preferred to permeability, for it can be directly measured from the operation of the plant. Impedance is defined as the pressure difference divided by the flow rate ($[Z]$ =Pa $\cdot$ s/l). From the eqn (2.1) it can be seen that it is inversely related to permeability, and is scaled by the characteristic dimensions of the reservoir and by the viscosity of the fluid,

$$Z = -\frac{\mu L}{A}\frac{1}{k}. \tag{2.13}$$

Also terms injectivity or productivity are used. They both equal the inverse of impedance and are thus proportional to permeability.

Chapter 3

Geothermal energy

Geothermal energy is the energy contained as heat in the Earth's interior (primordial heat and heat generated by radioactivity). Heat extraction from the ground warmed by the sun by heat pumps with horizontal piping located just beneath the surface is excluded from our definition. Due to poor thermal conductivity of soils, solar heat virtually disappears at depths greater than 20 m [8] and hence all heat at greater depths is considered geothermal. Geothermal energy can be utilized by exploitation of several kilometres of deep boreholes, which is of main interest of this thesis, but also by geothermal heat pumps with heat exchanger located some 100 m or so below the ground.

As the Earth was formed from stardust about 4,5 billion years ago, a vast amount of heat energy was released. A long time this energy was thought to be the only source of Earth's inner heat, but nowadays it is known that also decay of radioactive isotopes contributes to Earth's inner warmth. In order to generate noticeable amounts of heat, the isotopes have to be relatively abundant within the Earth and have half-lives of the order of the age of the Earth. Such long-living isotopes that warm the inner Earth noticeably include $U^{235}, U^{238}, Th^{232}$ and K^{40}. [9, 10]

Heat flows from the core of the Earth towards the surface, finally radiating into the space (the rate of cooling is faster than the rate of heating, and hence the Earth is still cooling down). Temperature rises when moving from the surface towards the core of the Earth. The dominant heat transfer process in the main body of the Earth is convection (the heat transfer due to the movement of matter). This is a very efficient form of heat transfer, resulting in rather small variations of temperature across the convecting layer. Due to decreasing temperature, the matter is too rigid to convect in

the outer 100 km or so of the Earth's crust and conduction becomes the dominant heat transfer process. This leads to larger changes of temperature, i.e., to larger geothermal gradients. [8]

Geothermal gradient is called the rate at which the temperature rises as a function of distance from the surface. The average gradient near the surface of the earth is about 30 °C/km, but at particular places (where geological sediments are rather young) it may be lower than 10 °C/km [10]. On the other hand, in areas of volcanic activity its value might be more than ten times the average. Most volcanic areas are found at boundaries of tectonic plates. [9]

A phenomenological conduction-rate equation (Fourier's law) states that

$$q'' = -k\nabla T, \tag{3.1}$$

where q'' is the heat flux ($[q''] = \mathrm{W/m^2}$), T is the temperature and k (defined by this equation) is the thermal conductivity ($[\mathrm{k}] = \mathrm{W/(m \cdot K)}$) [11]. Minus sign indicates the fact that heat flows from higher to lower temperature. Heat flow is thus affected by geothermal gradient (∇T) but also by thermal conductivity of the rocks. Values of thermal conductivity for most rock types are of similar magnitude, e.g. it ranges from 2.5 to 3.5 $\mathrm{W/(m \cdot K)}$ for sandstones, limestones and most crystalline rocks. [8]

At present there are no reliable *in situ* methods for measuring thermal conductivity of rock, and thus it is best measured in laboratory using core samples taken from boreholes. Temperatures (and thus gradients) are measured with quick and relatively inexpensive electrical thermometers in wells [10]. It should be pointed out that measurement of temperature in shallow wellbores can be used to predict, but definitively cannot guarantee the temperatures at greater depths. The only reliable temperature assessments today are the ones obtained by direct measurement at drilled boreholes. [12]

3.1 Geothermal systems

The high temperature within the Earth is by itself not enough to make geothermal energy viable - a geothermal system is needed. It consists of three parts: a heat source, a reservoir (or aquifier) and a fluid. The reservoir means a large volume of rock material

that has relatively high permeability and that is also at a reasonable distance from the surface. Usually the reservoir is surrounded by impermeable rocks, though it might still be connected to the surface by fractures and fissures. The fluid is water (in most cases meteoric water, meaning the water which rains down from clouds and penetrates down to the reservoir) either in liquid or vapor phase (or a mixture of them), depending on the site's temperature and pressure. As the heat of the reservoir transfers to the water, its density decreases. Because of that gravitation has a bigger effect on cold water, causing warmed water to flow upwards and colder to descend to the reservoir[1]. The warm water reaching the surface may cause geothermal activities, such as hot springs, geysirs, fumaroles and steam vents. [9]

Because the phase of water varies, the geothermal energy plants can be divided into two subclasses: liquid- (or water-) and vapour-dominating systems. In liquid-dominating systems the liquid water is the continuous, pressure-controlling fluid phase. Some vapour may be present, generally as discrete bubbles. Such geothermal systems have temperature from 125 to 225 °C and they are most widely distributed in the world. In vapour-dominated systems the fluid is usually a mixture of liquid and vapour, with vapour as the continuous, pressure-controlling phase. Geothermal systems of this type, the best known of which are Larderello in Italy and The Geysers in California, are fairly rare, high-temperature systems. [9]

In the surface the water's energy content can be utilized either by direct heating or by electricity generation. The efficiency of conversion of thermal energy to electricity depends highly on temperature, and thus the water temperature should be at least 150° for a geothermal electricity plant to be economically viable. In direct-use applications (district heat) lower temperatures can be used. [9]

Unlike many other sources of renewable energy, geothermal energy is independent of weather and time - it is practically always available, throughout the year, throughout the day [9, 10]. Geothermal plants can be operated at capacity factors[2] over 90 % [13].

Geothermal energy is utilized world wide and it is one of the most significant renewable energy sources. Its high availability distinguishes geothermal energy from many other renewables and due to this, geothermal plants can produce more power per given capacity. Total geothermal electricity producing capacity in 2005 was 9000 MW [14]

[1] Therefore convection contributes mostly to the heat transfer from the reservoir (not conduction, a mechanism typical to rocks with low permeability) [10].

[2] Capacity factor means the relative portion of time which the plant is operating. Capacity factor is 1 when plant is operating all the time.

and direct utilization capacity was 28000 MW [15]. Annual growth in the production is estimated to be about 10 % [8]. Especially the growing use of geothermal heat pumps usage contributes significantly to the present growth in capacity [15].

Countries with the largest installed capacities (and also annual energy production) are the USA, Sweden, China, Iceland and Turkey. The highest energies per population are reached in Iceland, Sweden, New Zealand, Georgia and Denmark. Though not in the "top five", also poor and developing countries such as the Philippines, Nicaragua, El Salvador and Costa Rica produce a significant part of their national energy by geothermals (e.g. 21 % of total electricity was produced by geothermal energy in the Philippines in 1996 [10]).

Finland, being far from tectonic boundaries and having a precambrian platform with a rather low geothermal gradient (8 - 15 °C/km [16]), does not have significant potential for conventional geothermal energy applications [17]. The HDR method (see chapter 4) can theoretically utilize the heat contained within the ground of Finland, but there are way more economical sites available. However, geothermal heat pumps do not require high temperatures and can thus be successfully utilized in Finland.

3.2 Renewability and sustainability of geothermal energy

Most renewable energy sources derive their energy from the sun, which has limited lifetime and thus limited energy content, but compared to human lifetime this time frame seems infinite and thus this energy is considered 'renewable'. That is also the case of geothermal energy - Earth's inner heat is plentiful yet confined. An estimate provided by the U.S. Geological Survey states that heat energy in the upper 10 kilometres of the Earth's crust in the U.S. equals 600 000 times the country's annual non-transportation energy consumption [8]. The technical potential (the amount of energy which can theoretically be extracted by using current mature technology [8]) for renewable sources are shown in figure 3.1. Therefore it can be stated that globally geothermal energy is essentially inexhaustible. From the local point of view, however, a particular geothermal plant can be depleted (cooling/pressure drawdown), and one of the main issues in planning a geothermal plant is to assess the lifetime of the geothermal field. Due to these reasons renewability and sustainability of the geothermal energy are somewhat complex concepts.

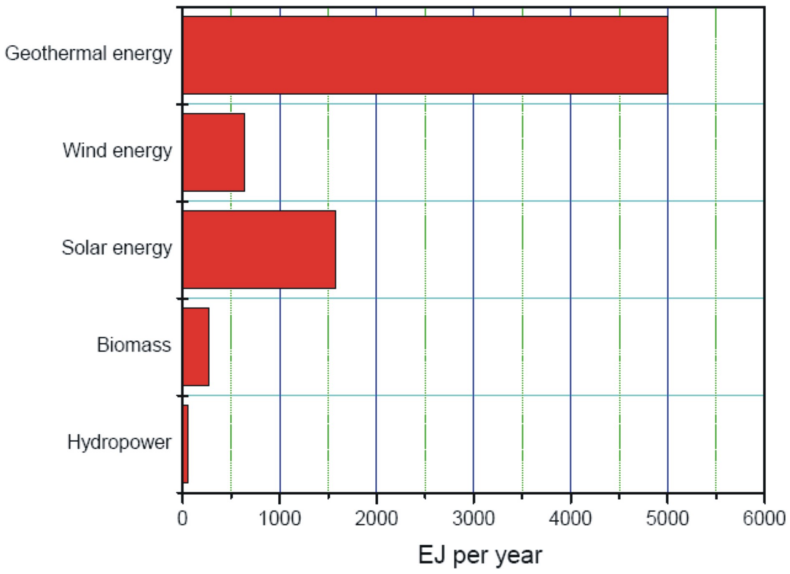

Figure 3.1: *Technical potential of renewable energy sources [18].*

The definition used in this thesis for renewability is "the ability to maintain the installed power capacity indefinitely without encountering any resource degradation" [19], and for sustainability it is "the ability to economically maintain the installed capacity, over the amortized life of a power plant, by taking practical steps (such as make-up well drilling) to compensate for resource degradation (pressure drawdown and/or cooling)" [19]. In practise, renewable capacity corresponds to natural heat recharge rate (conductive and convective) into the system and sustainable capacity is supported by extraction of stored heat in addition to natural inflow.

Empirical experience has shown that sustainable capacity is typically an order of magnitude greater than the renewable, which indicates that operation at renewable capacities is rarely economically viable. Also, it is likely that operating the reservoir at higher than renewable levels results in increased natural recharge heat rates into the system (due to cooling/pressure dropdown), which has been monitored in numerous plants. In addition, simulation strongly suggests that any resource degradation caused by typical plant lifetime of 30 years disappears in 100-300 years (pressure returns to its original level in the time frame of 30 years and heat within 300 years). Thus, no permanent damage is done to the reservoir. For these reasons, operating at a sustainable rather than renewable capacity level is favourable in geothermal plants. Even operation at a higher capacity level to rapidly recover the capital investments can be commercially viable at the beginning of the operation. [19]

Utilizing geothermal energy in a sustainable manner might require bringing new plants on-line while old ones are being depleted. Recovery of a geothermal field takes at most 300 years, whereas the renewal of e.g. fossil fuels will take millions of years. Thus it is actually the time frame that defines the renewability - geothermal energy is commonly agreed to be renewable whereas fossil fuels are not.

3.3 Environmental impacts

All energy production affects the environment due to some kind of engineering and building activity, and geothermal energy is no exception. Geothermal energy is generally considered as a clean and renewable source of energy, but nonetheless it has various (though controllable or minor) impacts on the environment. Such effects should be considered throughout power plant's exploration, production tests, construction and operation [20]. Environmental impacts of HDR geothermal power plants (introduced in chapter 4) differ somewhat from those of conventional geothermal plants and thus they are discussed in that section.

3.3.1 Physical impacts

Building a geothermal power plant (and required roads) and its operation has effects on the geophysics of the ground, of which most important is probably the land subsidence. When the extraction rate of fluid exceeds the inflow, the amount of fluid in the reservoir is decreased. This reduces the pressure in the pores of the rock, which lowers the groundlevel. There is evidence of land subside in almost every utilized geothermal area, but the magnitude of this phenomenon can vary significantly ($\sim$ 10 – 400 mm/year [21]). Water-dominating systems appear to subside more than vapour-dominating ones. Subsidence can be mitigated by the reinjection of spent fluids, which is done in most plants today [10]. Other possible physical effects are slumping or landsliding which may lead to destruction of local vegetation, which in terms causes additional erosion. Re-vegetation programmes, proper drainage for roads and modern drilling technology (reduced amount of land usage required) ease these problems [9]. Land usage of geothermal energy is low compared to other energy sources, since main processes take place below the ground level [22].

As geothermal plants tend to be located at areas characterized by natural volcanic activity and deep earthquakes, the contribution of geothermal operation to the seis-

micity of the considered area is not perfectly clear. Nonetheless, the injection of fluid (specially high-pressure fluid) back into the reservoir has been observed to induce seismicity. However, experience has shown that reinjection triggers a high number of low intensity events, favouring continuous release of stress instead of high-intensity (micro)earthquakes, which is considered to be a positive effect. [8, 10, 20]

Apart from temporary noise caused by construction and drilling activities and borehole maintainance, the noise caused by geothermal power plants can generally be kept at an acceptable level. Suitable muffling and silencers can be used to reduce the noise level further [9].

Because geothermal power plants operate at relatively low water temperatures, the efficiency of conversion of thermal energy to electricity is also quite low. Thus waste heat per unit power of electricity produced is quite large for geothermal plants. Waste heat is transferred to the environment through cooling towers and their main impact is at a local scale. Main consequences are a slight heating of the atmosphere and increased humidity, which possibly generates fog.

3.3.2 Impacts on air

A geothermal fluid has a chemical composition which depends on the local properties of the bedrock. The utilization of geothermal energy requires large amounts of fluids, thus leading to emissions to air (discharge of gaseous contaminants from wells during drilling and testing and gas exhausters of the power station [9]). This steam contains non-condensible gases, mostly carbon dioxide (CO_2), but also variable amounts of methane (CH_4), hydrogen (H_2), nitrogen, (N_2) ammonia (NH_3), hydrogen sulfide (H_2S) and mercury (Hg) [9, 23].

Some studies claim that exploitation of a geothermal field often reduces natural emissions from it. As the carbon dioxide emissions related to geothermal plants are not created by power production, the CO_2 released is present in the rocks, and that it is likely to be vented out anyway. Research of volcanic terrains suggests that development of geothermal fields does not change the amount of the total CO_2 emission. [8, 21]

Even when discounting this benefit, amounts of carbon dioxide emissions (major contributor to greenhouse effect) from geothermal fields (average 122 g/kWh [8]) are well below those of natural gas, oil or coal ($\sim$ 500 - 1500 g/kWh). Carbon dioxide emissions from different energy sources are shown in figure 3.2.

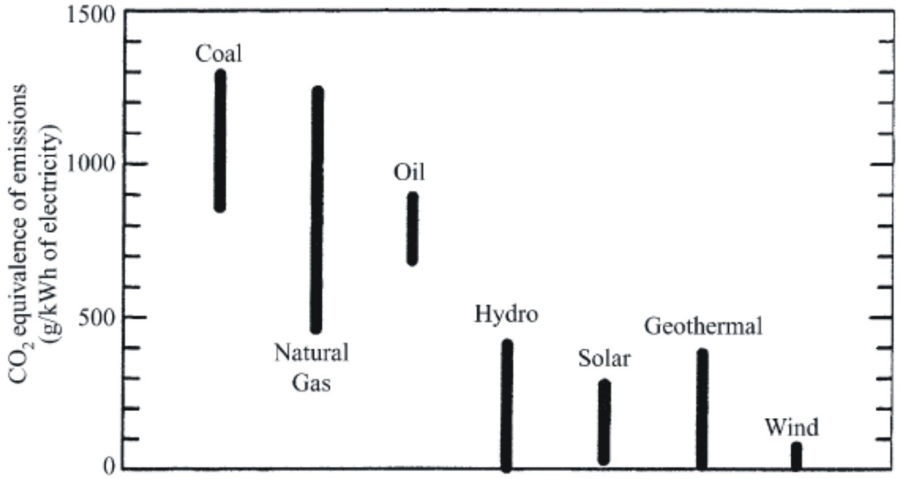

Figure 3.2: *Comparison of CO_2 emissions from different types of energy sources [20].*

Traditionally, geothermal plants have had a bad reputation due to unpleasant, rotten-egg-like smell of hydrogen sulfide H_2S. Hydrogen sulfide requires attention as it is toxic in moderate concentrations and has been proposed to be oxidized to SO_2, thus contributing to the acid rain problem. Still, this oxidation process has not been experimentally proved [21] and anyway the modern geothermal plants are equipped with chemical systems to trap and dispose H_2S.

Discharged mercury vapour is likely to be distributed over a wide area. It is known to accumulate in the food chain and have fatal effects on the nervous system in high concentrations. Amounts of mercury can be predicted from reservoir chemistry and monitored to assure that the national guidelines for air quality are not exceeded. If necessary, system for removing contaminants from gas exhaust may be implemented. [9]

3.3.3 Impacts on water

Because the fluid contains many pollutant chemicals and heavy metals, its disposal can lead to water pollution effects. The same chemicals as in the discharged gases are present in the fluids, but steam condensate will typically contain more volatile contaminants (dissolved gases) and waste water will contain more of the less volatile chemicals such as lithium, arsenic and boron, which all have an adverse effect on the environment. Concentrations of chemicals can be predicted by geochemistry of the reservoir and the fluid can be diluted to plain water (thus lowering the concentrations

to acceptable levels) before disposal. [9]

As is the case with many other problems of geothermal plants, water disposal problems can be overcome to a large extent by reinjection of spent fluid (today reinjection is almost always used) [8]. Groundwater contamination can be avoided by casing reinjection wells so that reinjected fluid cannot mix with groundwater [9].

Chapter 4

HDR

4.1 Concept of HDR

When utilizing geothermal energy, only the heat source has to be fully natural - the reservoir can be modified and extra fluid can be injected into the reservoir. After all, there are comparatively few locations on Earth where all three parts of a geothermal system are provided naturally. For example, the fluid flown to the surface can be reinjected back to the reservoir after heat extraction by special injection wells. Injection wells are already widely in use, and they have also been used to replenish and maintain old and exhausted geothermal plants [9]. Also the reservoir can be artificial. In many places the magma has intruded quite near to the ground level, producing a high geothermal gradient and heat flow, but there is no reservoir - there are only hot, dry rocks (HDR).

A reservoir is formed into rock material when high-pressure water is pumped through a drilled well (injection well) into a deep body of hot, compact rock at several kilometres of depth, causing its hydraulic fracturing (see section 4.3.1). The water opens up natural joints of the rock and increases its permeability permanently. The fracturing process is monitored by seismic measurements (see section 4.4.1). When the fracturing is done, production (extraction) well (or many of them) is drilled to intersect the reservoir, sufficiently far away from the injection well, and it is fractured in a similar way as the injection well to grant access to the already stimulated zone. When the wells are ready and the fracturing processes over, cold water can be pumped into the reservoir via the injection well, and extracted from the production well(s), where heat content of the water can be utilized. A schematic picture of an HDR power plant

consisting of two production wells is shown in figure 4.1.

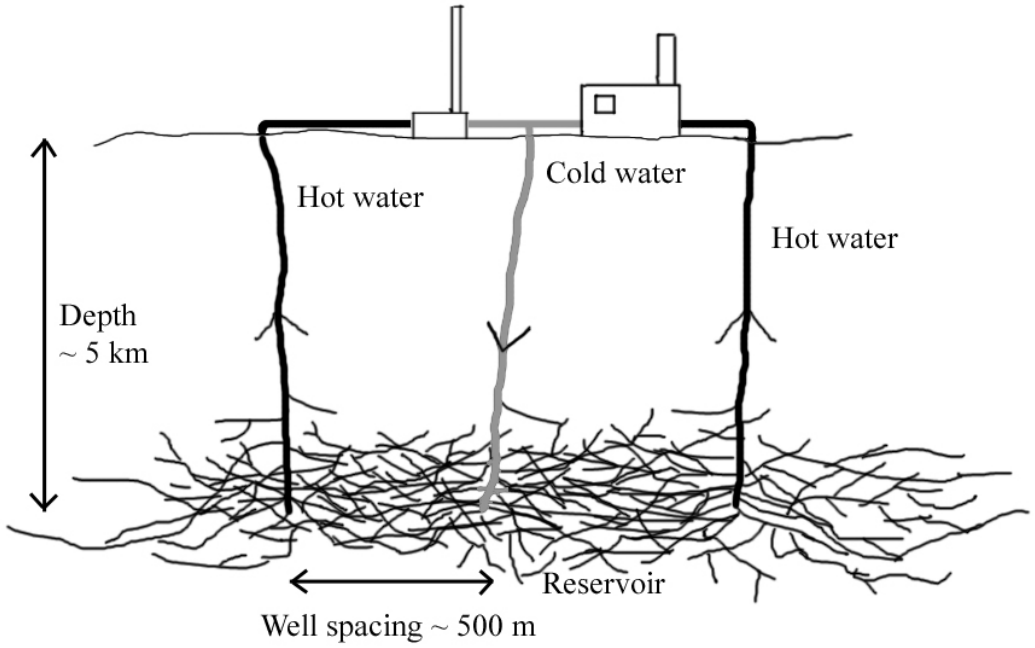

Figure 4.1: *Schematic representation of an HDR reservoir formed by artificial fracturing.*

Nowadays the term HDR refers not only to areas of hot dry rock, but also to associated projects and techniques used to generate reservoirs in such places [9]. The HDR techniques were first experimented in Los Alamos, New Mexico, USA, in 1970. After that, similar projects have taken place in Australia, France, Germany, Japan and the UK. The most important projects today are being carried out in Los Alamos, Rosemanowes (UK), Hijiori & Ogachi (Japan), Soultz (France) and Fenton Hill (New Mexico, USA).

There exists a diverse terminology describing geothermal reservoirs with varying characteristics. HFR (Hot Fractured Rock) and EGS (Enhanced Geothermal Systems) and Graben (refering to a geological setting of Rhine Graben in Europe, where e.g. the Soultz HDR site is located) mean more or less the same as HDR, while HWR (Hot Wet Rock) indicates the presence of water in or nearby the reservoir and the term hydrothermal system is used when water is abundant in the system. [10, 24, 25]

Classical geothermal plants are usually located at the boundaries of tectonic plates, where fluids and reservoirs are naturally present whereas HDR plants can be found anywhere where sufficient heat can be extracted. However, nowadays many conventional geothermal plants use procedures first associated with the HDR method (reinjection, hydraulic fracturing, seismic measurements). In addition, properties of geothermal fields are varying by their nature. Thus there is no distinct difference between concepts of conventional and HDR geothermal energy and the most widely used term

HDR can be misleading. The term EGS (Enhanced Geothermal Systems) would be scientifically more justified, but "the phrase 'hot dry rock' is too catchy to disappear easily." [8]

4.2 Field characterization

Research has shown that properties of a reservoir are strongly dependent on the site. Thus it is vital to characterize various properties of a given field before starting any construction activities. Fields are described by "regional and local geology, dating of rocks, surface manifestations of geothermal activity, heat flow measurements and geophysical exploration, including electric, seismic, gravity and magnetic surveys" [26]. Key parameters to be estimated are temperature, reservoir volume, permeability and also chemical composition of the rocks and the fluid. [10]

If there are surface thermal manifestations (such as fumaroles or hot springs) present, their properties are easily (and at low costs) determined and give essential information about the site's properties [10]. However, these phenomena are limited to areas of volcanic activity and thus are not often found at HDR sites.

Temperature, perhaps the most vital property of the planned site, is best measured by monitoring temperature in various test wells. Thermal history of the area (estimated by a model based on dating measurements) and ore deposit geology play an important role in this endeavor. Total available energy can be evaluated by extrapolating temperature profiles and by combining it with the surveyed volume of the reservoir. Improvements to temperature measurement tools in high temperatures would improve the reliability of these estimates. Temperature profiles can also yield information about the heat flow mechanism: linear temperature increase results from conductive heat flow, indicating presence of impermeable rock. [26]

A network of natural fractures seems to be commonly present within deep basement rocks, causing the permeability of the rock to be at least an order of magnitude higher than the permeability of the intact rock [27]. Exact properties of natural fractures of the reservoir determine the effect of hydraulic fracturing and the whole behaviour of the HDR system. While it is impossible to know these properties precisely, some information can be obtained from core samples taken from the drilled wells. The number of wells limits these data noticeably, and e.g. natural fracture size and mutual connectivities of fractures are very hard to obtain from the core samples. These properties of

the reservoir could be better obtained at a later stage of the development, but this is not an advisable approach, since these qualities should be known before construction of deep wells. [26]

Thus, a stochastic three-dimensional model to estimate the number density, orientation and size distribution of fractures is a necessary tool for field characterization. It has been observed that the natural fracture network obey a fractal size and density distribution, and nowadays a fractal approach to modelling is often preferred. Numerical modelling suggests that permeability enhancement due to the hydraulic fracturing is almost proportional to the fracture density. Thus the initial fracture density is a vital parameter to be estimated before the hydraulic fracturing is begun [28].

Besides spatial fracture orientations, the stress state of bedrock is one of the main factors affecting orientation of artificial fractures (due to hydraulic stimulation), and it can also give information about the anisotropic permeability distribution of the reservoir. Local geology, tectonic setting and monitoring of seismic events provide some information about the regional stress state. Because a commercial HDR plant should be operating at least 30 years, there is plenty of time for chemical reactions inside the reservoir to change reservoir characteristics. Dissociation/precipitation of minerals into/from hot water (depending on temperature, pressure and flow rate) may have fundamental impacts on flowing properties of the reservoir, and thus chemical evaluation of the reservoir rock is also included in the field characterization. [26]

When the field is proved to have potential as an HDR site, the construction of the HDR system can start. The first well (injection well) can be drilled into the rock material.

4.3 Construction of an HDR system

The objective of hydraulic fracturing is to improve reservoir permeability permanently as widely and uniformly as possible, preferring the deepest flow paths (due to greater temperature) and avoiding creation of flow short circuits (which would lead to premature temperature drawdown). Thus the aim of the fracturing is not only to increase permeability but also to increase the heat transfer area. Increase of heat transfer area (due to decreased fracture spacing) is vital in order to have significant positive effect on the plant's performance. [29]

4.3.1 Hydraulic fracturing of the reservoir

The reservoir is formed into rock material when high-pressure ($\sim$ tens of MPa's [30]) water is pumped through the injection well into a deep body of hot, compact rock, causing its hydraulic fracturing[1]. Pumping increases the pore-fluid pressure which opens up natural joints in the rock and causes the separated rock surfaces to slip past one another (fail, shear) according to natural stress conditions at that depth. In HDR projects the rock mass is typically fractured, and in such a case a high-pressure fluid tends to increase the apertures of existing fractures rather than create new ones [32].

Experiments have shown that pore pressure needed for seismic failures (critical pressure) increases with the distance from the surface. At the Soultz HDR site, the downhole pressure was slowly, gradually increased and thus every shearing event near the boreholes (located by microseismicity) could be linked to a specific pressure. The depths of such events as a function of pressure is shown in figure 4.2. This rise of pressure needed for fractures to fail as depth increased indicates the depth dependence of the stress field.

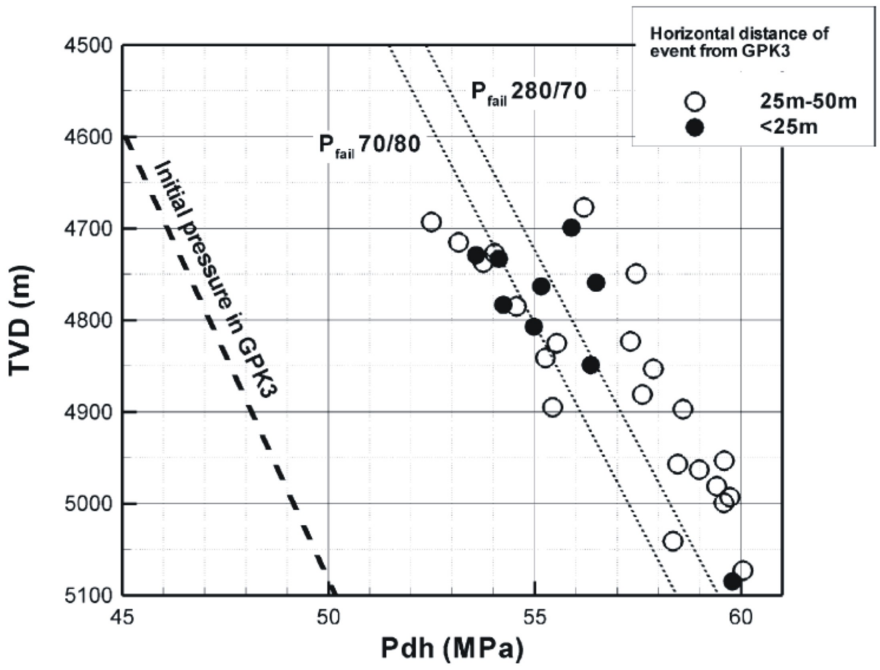

Figure 4.2: *Depths of microseismic events as function of a triggering pressure for borehole GPK3 at the Soultz HDR site. Dotted lines on the right represent theoretical estimations of the failure pressure for fractures in the borehole for two frequent fracture orientations. Numbers (70/80 and 280/70) indicate the angles of fracture orientations. [33]*

[1]Such a technique has been earlier studied and used in both oil and mining industry [31].

When the pressure is decreased, the rock blocks close together again, but not with the perfect match they had before - fortunately, an effect called natural or self-propping allows the fractures to keep partly open. Small gaps and fissures remain in the fractures due to rough characteristics of the displaced fracture surfaces [34]. Thus, permeability of the rock is increased permanently. This process causes emission of seismic waves, which can be monitored, providing access to the mapping of stimulated zones.

In addition to the self-propping, the proppants (small particles, e.g. sand grains [35]) can be added into the injected fluid. When fluid enriched with proppants flows into fractures, proppants are stuck in them and keep them opened even when the pressure is dropped again. Such a procedure was successfully done in Rosemanowes, but the cost of appropriate proppants is relatively high and their penetration depth is quite limited.

The operating pressure is typically of the same magnitude (though smaller) as the stimulation pressure. Thus rock blocks would not be totally closed even without self-propping, thus assisting the permeability of the reservoir material to remain relatively high.

Furthermore, there might be natural large, permeable faults in the reservoir, which are unlikely to be intersected directly by a borehole, but as the stimulation process proceeds, these faults tend to be intersected by the newly created fissures and stimulated natural fractures [36].

It has been proposed that it could be a viable approach to keep the downhole pressure during the operation so high, that the hydraulic fracturing would slowly continue and the reservoir would keep growing. When the old parts of the reservoir would cool down, the new production wells could be drilled into newer parts. [37]

4.3.2 Parameters for controlling the fracturing

To successfully fracture the reservoir, the failure pressure of fractures should be estimated. The downhole pressure (and thus opening of fractures) can be controlled by proper choice of various parameters: injection flow rate, injection pressure, total injected volume (duration of injection), fluid density, viscosity, temperature and fluid additives (proppants) [38]. In this section these parameters are reviewed from the viewpoint of the hydraulic fracturing, but they naturally have similar effects during the operation of the plant.

Density difference between the injected fluid and the reservoir fluids results in dissimilar stress distributions in the fractures and it also affects the flow paths which the fluid takes. Thus the number of shear events and their distribution is affected by fluid density, and computer models have been developed to estimate these effects. A numerical study of the Soultz HDR reservoir shows that denser fluids are likely to flow towards the bottom of the reservoir (hottest part) and thus the average depth of shear events is greater. Also, a larger number of shear events was observed when using a denser fluid. Density of water is most easily influenced by dissolved solids (also the temperature contributes). Typically, water rich in NaCl (heavy brine) with a density up to ~ 1200 kg/dm^3 can be used instead of fresh water. [39]

Temperature of the injected fluid has a slight effect on its density[2], but it affects the fracturing also by other ways. Cooling reduces the total stress of the rock mass, which can lead to aperture growth and thus to increased permeability [55]. Effects of temperature take place typically quite slowly and thus their impact on long-term performance of the reservoir is of greater importance (discussed in section 4.6.1).

Increasing the flow rate of the injected water increases the downhole pressure[3] (pressure in the reservoir), which determines the opening and shearing of fractures and thus the injectivity enhancement. At the Soultz HDR site, the relationship between the injection flow rate during fracturing and the post-fracture injectivity was found to be almost linear (figure 4.3).

Modelling suggests that a sudden, stepped, strong high-rate stimulation results in a more efficient fracturing than slowly increasing flow rate [41]. Typical injection flows along with the pressure responses are shown in figures 4.4 and 4.5. This kind of approach has been found to be a practical way to fracture the rock mass, but it can also provide information about reservoir's properties. At each step the flow rate is kept constant until the downhole pressure saturates. With increasing flow rates, fractures start to dilate. They keep extending as long as the pressure in the fractures is high enough to allow it, but at some point, as the distance from the injection well increases, the pressure is decreased below that limit. Then an equilibrium is reached, and the water loss equals the injection flow rate. This phenomenon can be seen in the pressure cycles of figures 4.4 and 4.5.

After saturation the flow rate is set to a greater value, and this process is repeated as

[2]for pure water density ranges from 958 kg/m^3 (100 °C) to 1000 kg/m^3 (4 °C) [5].

[3]At the Soultz HDR site this relationship (downhole overpressure vs. injection flow rate) was found to be quadratic (overpressure was proportional to the square of flow rate) before the maximum pressure was reached.

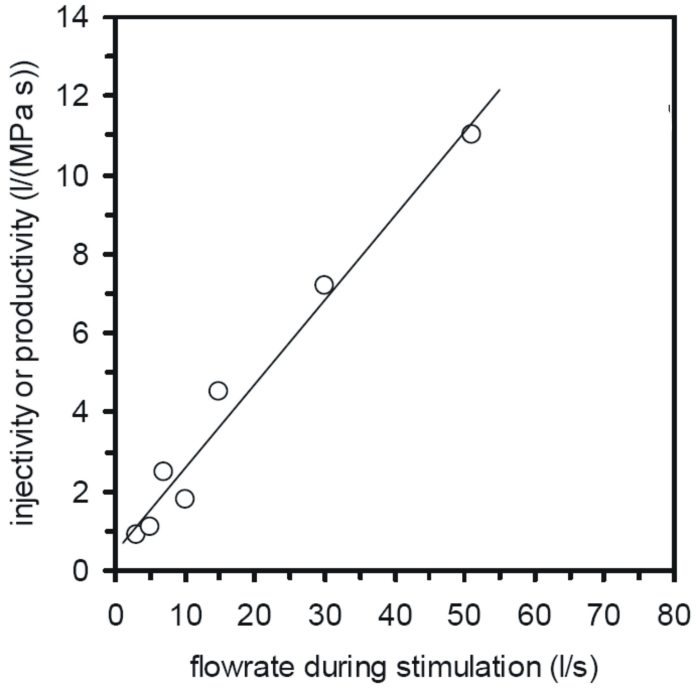

Figure 4.3: *Injectivity after fracturing was linearly related to the stimulation flow rate at Soultz HDR site, wellbore GPK-1, 1993 [40].*

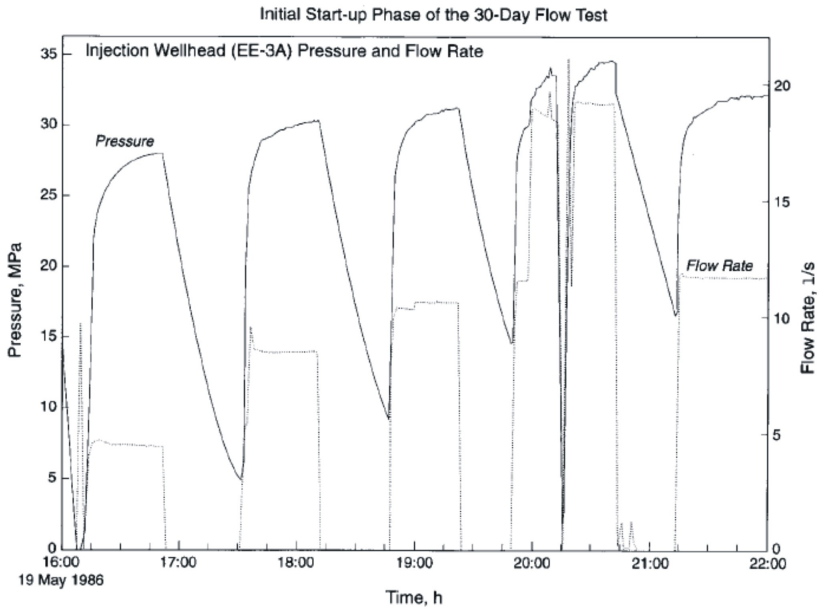

Figure 4.4: *Downhole pressure and injection flow rate as a function of time (pressure response) at the Fenton Hill HDR site [36].*

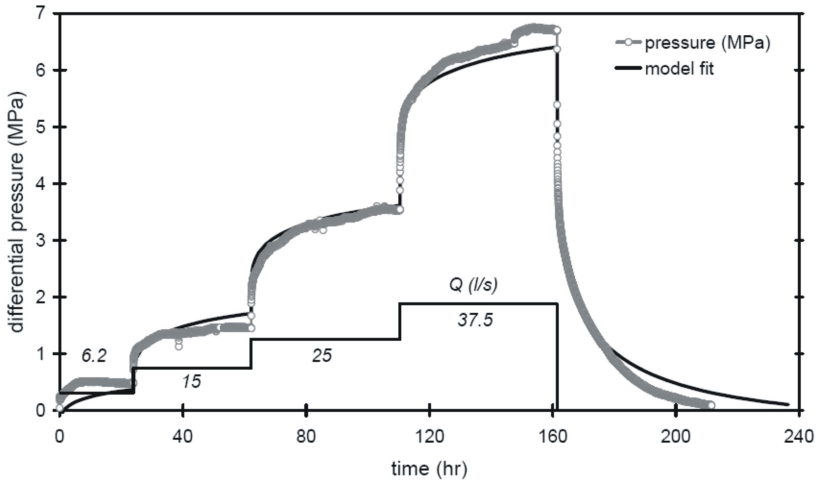

Figure 4.5: *Downhole overpressure (observed and modelled) and the injection flow rate of the well GPK-2 at the Soultz. Quadratic behaviour indicates presence of turbulent or non-Darcy flow. [40]*

long as needed. Between pressure steps there might be time when injection is stopped, to let the reservoir stabilize properly, as in the case of figure 4.4. A graph of saturation pressure versus flow rate can be used to obtain information about the reservoir. For low flow rates, this relationship should ideally be linear, indicating laminar flow. For higher flow rates the flow becomes turbulent or non-Darcy, and the relationship is likely to be quadratic (relationship of this type was observed at Soultz, figure 4.5). If the flow rate is still increased, fracture dilation becomes a significant effect, and the pressure saturates. The shape of the saturation pressure graph yields information about the impedance, significance of turbulence, fracture dilation, water losses and flow geometry.

The underground reservoir created in this way contains a relatively small amount of water dispersed over a high volume of rock of higher permeability than in the surrounding, the large surface area of the rock making it efficient for heat transfer. The shape of all HDR reservoirs created to date have been highly elliptical. This is consistent with our knowledge of the stress fields in the earth's crust [12].

4.3.3 The production well

The seismic information (discussed in section 4.4.1) is vital when planning to drill a production well - another borehole at some distance from the first, injection well. It is vital not to drill the production well before the reservoir is created and its properties

are characterized, since they cannot be reliably predicted beforehand. The distance of these two wells should be large enough, allowing a large heat exchange surface area and thus a long operating lifetime of the plant. In particular, a large enough distance prevents the creation of short circuit between the injection and production wells, which would lead to rapid thermal drawdown. Well separation should be of the same order as the characteristic radius of the stimulated region, at least 500 m for an HDR plant of commercial potential. Increasing this distance seems to be a reasonable way to improve the productivity of an HDR plant [12].

At the newest phase of the Soultz HDR site the distances between adjacent wells have reached a value of around 600 - 700 m at a depth of 5 km [42]. However, the land usage was minimized and operation optimized by directional drilling: at the surface the wells are separated by not more than 6 m [43]. Once a production well is drilled, it is stimulated in the same way as the injection well, to improve access to the already stimulated zone. [25, 44]

Experiences with HDR pilot projects have shown that it is profitable to use (at least) two production wells instead of one (a three-well configuration), placed at opposite ends of the long axis of the reservoir [12, 37]. Such orientation of wells not only limits the amount of water losses (water flows into the production wells instead of permeable regions of the reservoir) but also permits the use of high injection pressures. This high pressure opens the natural fractures of rock blocks, thus reducing reservoir impedance. For these reasons, the installing of a second production well increases the reservoir productivity significantly compared to the case of one production well (modelling suggests that productivity would be increased by a factor of 4 in the case of Fenton Hill and by at least a factor of 3 in Soultz [43]).

4.4 Estimation of reservoir's properties

In order to create a reservoir with desired properties, its characteristics should be estimated before (field characterization, section 4.2), during and after the hydraulic fracturing. Key tools used for this purpose are seismic and borehole measurements, tracer tests and modelling.

4.4.1 Seismic and borehole measurements

During hydraulic fracturing it is vital to control reservoir's size and orientation. In every HDR project the fracturing process has been monitored by seismic and borehole measurements, which provide the only reliable evaluation of reservoir's characteristics. The monitoring process should begin before the hydraulic stimulation, thus enabling sufficient data of the evolution of the reservoir.

Seismic information is best obtained by installing a number of seismic measurement devices at known distances from each other (seismic network). For the measurements to be reliable, the seismic network has to be calibrated. This can be successfully done by thermally insulated explosives and sparkers (with known properties) placed in the boreholes. Due to high temperature, seismic sources which can operate at high temperatures are needed. The energy of such sources should be high to allow seismic observation stations to properly record their signals. A seismic network should consist of as many measurement stations as possible to improve the quality and reliability of the results. Both passive (measuring effects of hydraulic fracturing) and active (producing own seismic signals which can be measured) seismics have been used to evaluate properties of the reservoir. [45]

Microseismic data obtained from measurements done in the surface provide a map showing the locations of seismic sources (microearthquakes), which are interpreted to be the locations of the fractures which have failed seismically due to increased pore fluid pressure (shearing of pre-existing fractures). Generally a seismic zone is a region of higher permeability, but reservoirs are too complex and unique to enable generally valid interpretations. Complex models have been developed to properly explain the physical meaning of seismic events. By such a model (with appropriate seismic source parameters) the behaviour of individual fractures can be estimated. [32]

Several methods to measure physical properties of the reservoir via boreholes have been developed and tested. While they provide valuable information about physical quantities near the wellbore, they generally cannot provide complete data on the properties of the whole reservoir. Borehole measurements suffer from high temperatures present, because the operation of silicon-based semiconductor electronics is limited by a rather low temperature maximum ($\sim 175°$). [45]

By these measurements the volume, direction and shape of the reservoir can be estimated. Although evolution of the mapping technology and modelling methods have considerably improved the quality of interpretation of these measurement, there is

still need of better understanding of slips along faults and joints and their effect on permeability. [30, 32, 45]

Due to the complexity of the processes involved and the effect of local conditions, prediction of reservoir growth based on hydraulic parameters can be done only to a limited extent. Experience has shown that real-time monitoring and immediate response to the observed behaviour are more important than careful design and prediction. Combined seismo-hydraulic analysis carried out continuously in the field seems to provide the most promising approach for generation of a viable reservoir today. It is common that stimulation strategy is changed a few times during the fracturing in response to the actual behaviour of the system. In order to process vast amounts of data in near-real-time, seismic software have been developed, and in addition to seismic measurement devices, they play a key role during the creation of a reservoir. [34]

4.4.2 Tracers

In addition to seismic measurements, valuable information about reservoir's characteristics can be obtained by means of tracers. Special tracer substances[4] with good detectability are mixed with injected water and pumped into the reservoir. In the production well their concentration is assessed as a function of time. An example of a tracer concentration measurement is given in figure 4.6.

These tests are normally executed to estimate the size of the reservoir, its time-dependence, properties of different flow channels and fluid exchange rate. Breakthrough (produced volume flow at first appearance of the tracer) and median volume (produced volume when 50% of the tracer has been recovered) are the most useful direct measurements obtained from tracer tests. If the geothermal field has more than two wells, tracers provide information about types of flow paths between different wells (as for Soultz HDR site) and can be useful when evaluating the three-dimensional orientations of reservoir's fractures. Typically tracer testing takes significant amounts of time (from months to years), but it can be carried out simultaneously with plant's operation. [25, 46]

Both inert and reactive tracers are used. Inert tracers should be thermally and chemically stable to remain unchanged in the reservoir. Reactive tracers are either thermally

[4] e.g. radioactive substances, halogen salts, coloured dye or organic tracers such as Na-benzoate or benzoic acid [36, 46].

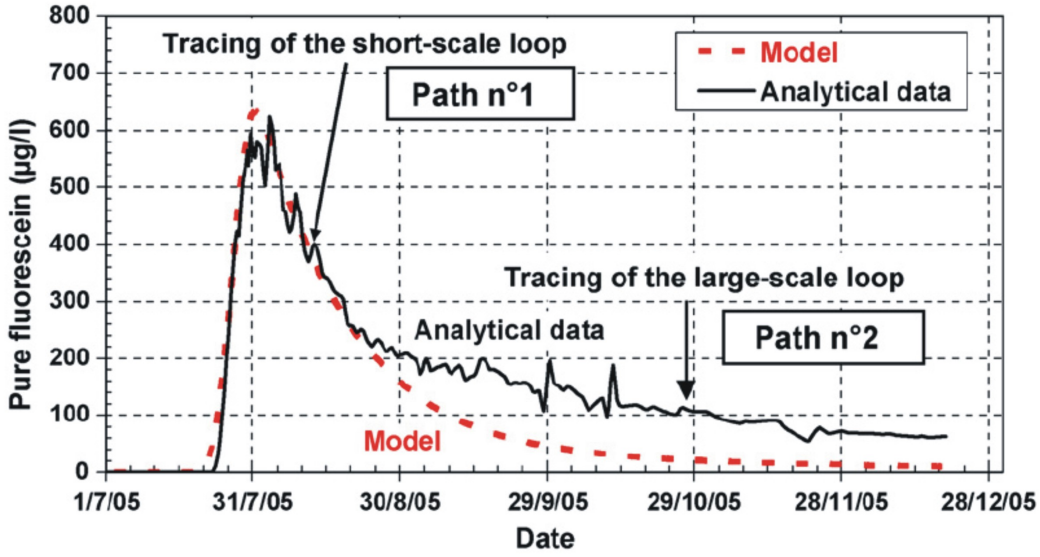

Figure 4.6: *Example of tracer recovery graph from Soultz HDR site. Graph indicates (mismatch between analytic data and model output in the later stage of the process) that there is another flow path with smaller mean velocity besides the dominating one [46]*

or mechanically sensitive (sorbing) - those that undergo an irreversible chemical transformation at a known temperature and those that attach themselves to crack surface. Temperature-sensitive tracers could be used to estimate the temperature profile of the reservoir. Usage of sorbing tracers simultaneously with inert ones could result in evaluation of the heat exchange surface area of the reservoir. [36, 47]

Another advantage of tracers is that they principally detect all flow paths within the reservoir, including joints that are in such a direction with respect to the stress field that they are practically aseismic (cannot be detected by seismic measurements) [37].

4.4.3 Modelling

Geothermal systems are varying in their properties, and their operation is affected by a number of geological, physical and chemical factors. Any attempt to model HDR plant's performance even adequately will lead to complex and wide mathematical and modelling problems and it has been stated that no model can properly simulate all properties of HDR plant decently. Secondly, the lack of reliable input data of the reservoir complicates the modelling process. [48]

Despite these difficulties, numerical simulation of the geothermal system is a crucial tool for understanding its behaviour. Models have developed along with an improved

understanding of geothermal fields and rock mechanics and with advances in computational techniques. Modelling is routinely used in HDR system development to predict both the effects of hydraulic stimulation and the long-term behaviour of the reservoir.

Models trying to predict effects of hydraulic fracturing use today fractal concepts to simulate a natural fracture network. To verify the reliability of such model, some real variables should be assessed. Methods like observation of fractures in core samples, X-ray tomography using a contrast medium as a tracer and permeability tests on rock samples can be useful. [26]

Models simulating the long-time behaviour of the reservoir are generally complex three-dimensional models, and they are able to handle a multiphase flow that is a mixture of water, carbon dioxide and NaCl (major components in many geothermal fluids). In these models thermoelastic effects and/or basic chemical reactions (precipitation/dissolution) are taken into account. More sophisticated models which simulate multi-species chemical reactions between aqueous, gaseous and solid species, do not take into account flow and transport effects.

The models are at most as reliable as the data used to develop them. At present the thermodynamic data for subcritical to supercritical water are insufficient. Models developed for geothermal reservoir simulations have also applications in other related research areas such as nuclear waste storage. [26, 47]

4.5 Operation of an HDR plant

Experiments done at the Soultz HDR site show that thermal properties of the system have a highly non-linear dependence on the geological and mechanical properties of the rock mass in which the system is created [48]. Due to pressure-dependent opening of joints and fractures, also the reservoir porosity and permeability are strongly pressure-dependent. Permeability may vary several by orders of magnitude when comparing the operating and the depressurized state, making the operation of an HDR plant hard to model. Therefore the reservoir is often characterized by operational parameters (parameters that can be measured directly) rather than scientifically defined, hydrological parameters [36]. The most important operational parameters are impedance and water losses.

4.5.1 Impedance

One of the most important parameter of the reservoir is the so-called flow impedance, Z. Impedance is defined as the difference between the injection and production well pressures divided by the produced flow rate ($[Z]$ =Pa $\cdot$ s/l). Basically impedance is just a scaled inverse of permeability, as discussed in chapter 2.

The impedance of wells consists of two parts: the first is the frictional resistance to flow (which can be estimated with pipe friction equations and friction factor-Reynolds number correlations) and it is usually very small (for example, for a typical HDR plant well impedance is 4 kPa s/l whereas the impedance of the reservoir is 1 MPa s/l). The other part of impedance of the wells forms from temperature-differences. As the operation of the plant continues, temperature of the whole injection well starts to approach the value of cold water injected into it whereas in the production well temperature approaches that of the reservoir. This causes density differences, resulting in a pressure gain (so, the contribution of this part to impedance is negative) in the fluid. However, typically this gain is less than 1 MPa and also this is usually rather insignificant when comparing to pressure loss in the reservoir. Thus the dominating term in the overall impedance is by no doubt the reservoir itself [36].

Turbulence, non-Darcy flow (flow that does not obey Darcy's linear law) and pressure-dependent movement of the fractures inside the reservoir result in a non-linear relationship between flow and pressure. The reservoir impedance tends to decrease with respect to increasing pressure, as shown in figure 4.7. It is evident that the overall impedance can be quite complex, but it can be divided into three components: inlet, main reservoir and outlet impedances.

The inlet impedance is caused by high concentration of streamlines and high velocities when inlet water enters the reservoir. This could lead to high pressure losses, but because the inlet pressure is often close to that of hydraulic fracturing, the opening of joints and fractures in the reservoir greatly offsets these losses. The main reservoir impedance consists of friction due to water flowing in the reservoir. The streamlines of the flow have diverged and velocities are low and even though flowpaths are rather long, pressure losses due to the main reservoir impedance are relatively small.

The last part of the impedance, the outlet impedance is similar to the inlet impedance, streamlines converging and causing pressure losses due to high velocities and non-Darcy flow. In addition, because the production well is usually maintained at a low pressure, fractures in the rock blocks are more tightly closed, increasing the impedance. Thus

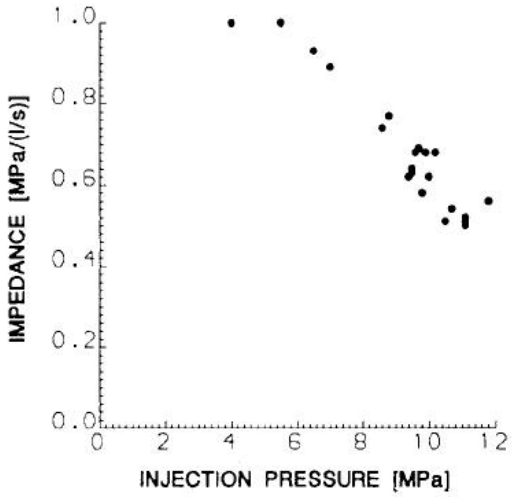

Figure 4.7: *Impedance as the function of pressure, Romanowes, UK [36].*

the outlet impedance is the most significant factor in the reservoir impedance. Due to that, it is reasonable to create large reservoirs: the spacing between injection and production wells can be increased without significant increase in the impedance.

There are some methods which attempt to decrease the large outlet impedance. Proppants can be injected down the production well to keep fractures opened [12]. Also, the pressure in the production well can be increased resulting in a drop in the outlet impedance, but that will also decrease the pressure difference over the reservoir, which decreases the volume flow through the reservoir (and high pressure in the production well i.e. *backpressure* also tends to increase water losses) [36].

Overall impedance should be less than 1 MPa · s/l for the reservoir to be technically viable (so that pumping requires less energy than can be produced). Almost all of today's HDR plants reach this value. It has been estimated that for an economically viable reservoir the overall impedance has to be less than 0.1 MPa · s/l (Soultz is about to reach this limit [43]). [36]

Ideally impedance should be so low that the primary concern limiting the operation of the plant would be thermal drawdown instead of the impedance [12].

Geothermal plant can be operated either in a pressure- or flow-controlled manner. Impedance links these parameters (pressures and flow rate) together, although the value of impedance is pressure-dependent. It is technically easier to operate the system at a constant pressure, and modelling suggests that it also results in a slightly improved performance [50].

4.5.2 Water losses

Ideally all the water injected into the reservoir would come back through the production well, thus forming a perfectly closed loop. That is rarely the case in the actual power plants, and thus water losses in the reservoir must be considered. The rate of water loss also equals the rate at which extra water must by added to the system. In places, where there exists a risk of provoking a damaging earthquake by high water losses, or in places with lack of water, water losses become of noticeable significance. Water also carries thermal energy out of the system, thus possibly accelerating thermal drawdown of the field. Amount of water losses depends on the size of the reservoir, the pressure used and the permeability of the surrounding rock.

Reservoir water losses can be divided into three components. First there is time-dependent water loss caused by permeation of water from pressurized joints into the micropores of the reservoir rock blocks. This water loss tends to decrease with time at any given pressure, because rock pores become saturated with water [51].

The second part of water losses is called an apparent water loss, as it is not actually a water loss. While hydraulic fracturing stores water in the expanding reservoir, a large part of it is recovered when the reservoir is depressurized. However, permanent changes in the fractures of rock blocks allow part of the water to be stored permanently.

A third component in water losses appears when faults and fractures intersect the engineered reservoir region, thus allowing water to flow out of the reservoir. This appears to be happening at Hijiori, whereas Fenton Hill seems to be well-isolated.

Water losses can be mitigated by installing a downhole pump in the production well. This kind of pump has to be carefully designed since it has to stand harsh conditions: high temperature and pressure and an aggressive chemical environment. A downhole pump not only reduces water losses, but it also eases the water flow to the surface and helps to maintain the pressure. It is advisable to including a scale inhibitor below the pump to protect the pump and the production well from unfavourable effects of precipitation of $CaCO_3$ [52]. At Soultz the water losses have practically disappeared when using downhole pumps.

Water losses tend to increase with increasing pressure (whereas the impedance decreases as shown in figure 4.7) as shown in figure 4.8. The optimal pressure can be reached at some point, where both the impedance and the water loss are tolerably small. Where water is adjacent, it might be reasonable to use high pressure and allow high water

loss, and if water resources are low, it might be sensible to use lower pressures, thus accepting a rather high impedance. [36]

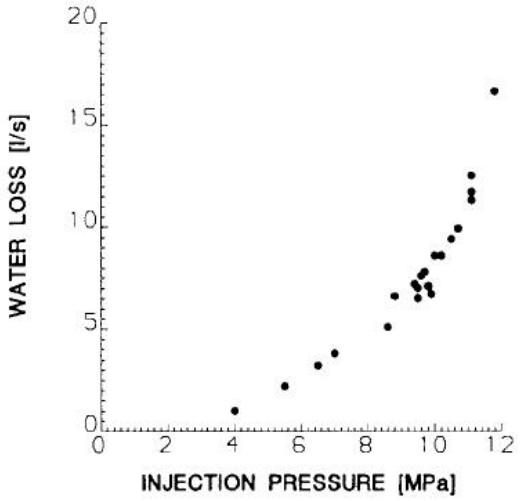

Figure 4.8: *Water loss as a function of pressure at Rosemanowes, UK [36].*

4.6 Time-dependent permeability

As geothermal plants are designed to stand at least for 30 years, the long-term behaviour of the reservoir must be given thought. When cold water is continuously pumped into the reservoir, the rock mass is eventually cooled down (especially near the injection well). Changes in flow properties caused by this cooling are called thermoelastic effects. Secondly, chemical reactions play a key role. Precipitation and dissolution of fluid may also have remarkable effect on the porosity and thus on the permeability.

4.6.1 Thermoelastic effects

Due to heat extraction, the reservoir will cool with time. This results in thermo-elastic stresses which can have both desired and undesired effects on the system's properties. Cooling reduces the effective normal stress, which in turn decreases the impedance of cooled flow paths. While the stress is reduced at the cooling zone, the shrinking rock is likely to pull exterior rock, thus causing compressive stress on the rocks surrounding it, resulting in slightly increased stress. [53]

Near the injection well a cooling of the rock results in changing of stress and in displacements within the rock. These changes increase the fracture aperture and thus the permeability. This effect diminishes with increasing distance from the injection well. This is to be expected, because the greatest cooling occurs at first near the injection well. The higher the fluid velocity, the greater is the part of the reservoir where increasing fracture apertures appear. [54, 55]

As the permeability of the cooled flow paths increases, there is a risk that the flow is concentrated on the cooled paths, thus lowering the output temperature. Generation of such short circuits is highly unfavourable, and much effort is being carried out to avoid it. For example, increasing the reservoir size decreases the probability of short circuit formation. A natural change in flowpaths due to thermal effects has been detected at many HDR sites [12], but more data is needed to evaluate the significance of this phenomenon. [27]

Contraction of the rock can also result in thermal cracking - creation of new fractures (perpendicular to the original one [56]), which would improve the flow properties. Whether this effect is important or not is primarily dependent on the in-situ stress conditions. [27]

Thermoelastic effects take place quite slowly, in a time scale of years, and thus they can normally be neglected when considering hydraulic fracturing.

4.6.2 Chemical water-rock interactions

The amount of water-rock chemical interactions (WRCI) and their effect on reservoir's properties are mainly determined by computer models. This is due to the complexity of measurements and to the long time-scales that these processes take. In fact, the long-time behaviour of a given field should be estimated already at the stage of field characterization, before drilling activities. Models can predict changes in porosity quite reliably, whereas predicting a change in permeability requires knowledge of precise properties of the rock [57].

Chemical reactions considered in such models are precipitation and dissolution. The type of these reactions depends on the chemical composition of the reservoir. Whether precipitation or dissolution happens, and to what extent, depends highly on the temperature, pressure and the flow rate. As these properties (specially temperature) do not remain constant in the reservoir, chemical reaction rates are also functions of distance

from the injection well to the production well. As such, WRCI are highly site-specific and general guidelines are hard to draw. WRCI might a have positive, negative or neglible impact on the overall impedance of the HDR plant. For example, at the Hijori HDR site, WRCI does not have any significant impact, whereas at Soultz, these reactions play an important role [57].

Temperature and pressure affect the chemistry in two ways: first, the solubility (saturation concentration) of a given chemical is a function of them, and secondly, the reaction rate depends on them. Flow rate has an obvious influence: the higher the flow rate, the more chemical reactions happen. Make-up fresh water can be added to the injected water, which has the potential to promote dissolution of chemicals and thus to increase the permeability. However, due to low solubility of cold water, modelling suggests that only high temperature fresh water has a significant impact.

As the injected water interacts first near the injection well, the dissolved amounts and thus the permeability increase are at first (still after $\sim$ 5 years of production) greatest near the injection well. The prediction of porosity and permeability changes at the Soultz HDR site after 5 years of production is presented in figure 4.9. However, this injection zone is eventually cooled down, which slows down the chemical reactions and at some point dissolution near the production well starts to dominate (after $\sim$20 years)[58].

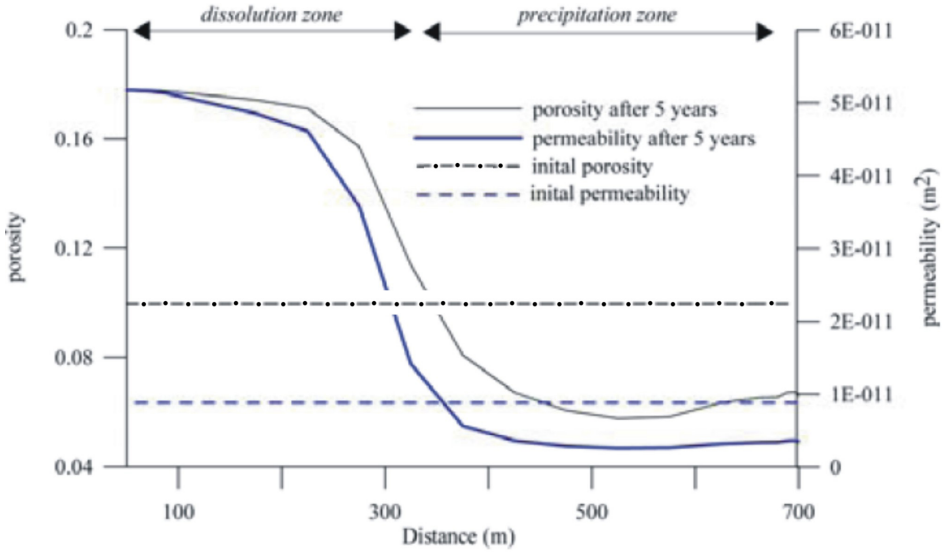

Figure 4.9: *Evolution of porosity and permeability after 5 years of exploitation, showing porosity and permeability increase near the injection well and decrease at the production well (model prediction) [59].*

As precipitation decreases the permeability and thus the productivity of an HDR plant,

two strategies have been presented to dissolve them. At first, injection of an acid (e.g. HCl) has been proposed. Modelling implies that it can be a successful approach. Also reverse circulation has been suggested. This means that the role of injection and production well is swapped for a period of for example one month. Cold water is injected via production well and extracted from the injection well. This procedure is likely to equalize properties of the reservoir (e.g. dissolve the acummulated precipitations near the production well) and thus improve reservoir properties. [59]

High initial temperature of the rock results in high rate of reactions (dissolution) and thus in increased permeability. Cooling slows down this effect, and this increase of permeability is modeled to be quite rapid (less than 10 years) after which it saturates. Increased permeability between the injection and production wells can also result in decreased water loss. The greater the reservoir (well spacing), the more slowly the cooling occurs. Thus, WRCI remain at a high rate for a longer period and have a bigger effect on larger reservoir.

As a commercial HDR plant requires quite large reservoirs and high temperatures, WRCI are likely to have relevance to the long-time properties of such a plant.

4.7 Environmental aspects

Another advantage of HDR is environmental aspects. As the circulation of fluid can be formed as a closed loop system, there is no (or neglible amounts) of pollution escaping from a power plant. As D. V. Duchane comments results obtained in the HDR pilot facility at Fenton Hill [51], the circulating water contained some amounts of dissolved solids, but their amount rapidly reached an equilibrium as the operation continued and the amount was quite insignificant. There are also low levels of dissolved gases (mainly CO_2) in the circulating fluid, but no gaseous emissions to the atmosphere occurred during normal operation of the HDR system. In addition, tests showed that it is possible to increase the power output of an HDR power plant by as much as 60 % within a period of about 2 minutes (and to maintain that level of production for at least 4 hours). These tests showed the important flexibility of HDR energy, which makes it possible to provide load-following output power [51].

Chapter 5

Permeability measurements

As an example of the ways an important reservoir property, permeability, can be measured, the permeability of 21 rock samples from Kaali meteor crater, Saaremaa, Estonia were measured. Motivation for these measurements came from Tartu University, where the effect of meteor impact on the properties of rock matrix is studied. Thus the rock samples themselves were not related to geothermal energy. From the viewpoint of this thesis, the measurement process itself, and the relation of permeability with other rock characteristics, are the main issues.

The rock samples were cylinders with circular cross section. Diameter of cross section was approximately 25,3 mm but the lengths of the samples varied from 21,5 mm to 25,7 mm. The ends of the samples were generally not parallel, and thus the lengths of the samples were approximated by their average lengths.

5.1 Equipment

Measurement equipment consisted of a sample holder, helium source (helium container of the physics department), nitrogen source (a nitrogen container of the measurement room), a vacuum pump, flowmeter, pressure meters, helium sniffer (leak-rate detector), injector with selector valves and of the capillaries and pipes connected them. In addition, there was a vacuum oven for preserving and drying the samples.

The sample holder was a rectangular aluminium slab, slightly wider than the sample. In the middle of the slab there was a round hole with a slightly greater diameter than

that of the samples. The slab had been split in two in the middle, and the two pieces could be tightened with the screws. A schematic representation of the sample holder is presented in figure 5.1. The cylindrical rock samples could be stuck into this sample holder, where both of their ends were left open for diffusive motion of fluids.

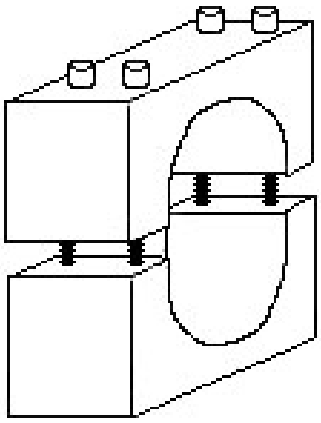

Figure 5.1: *The sample holder.*

The two ends of the sample holder were called injection side (from where the helium gas was coming) and flushing side (where the nitrogen flushed the surface of the sample and the flushing gas was lead to the helium sniffer). From the injection side the disc was sealed by a thick, round aluminium disc, with a chamber of 5 ml volume carved into the middle of it. There was a capillary into the chamber for inflowing helium gas (the left disc of figure 5.2). On the other side of the slab (flushing side) the sample holder was closed by a thinner aluminium disc which was intersected by two capillaries - one for the incoming nitrogen and one for the outgoing (leading to helium sniffer) mixture of nitrogen and helium (the right disc of figure 5.2). Both discs had four screwholes so that the whole holder could be tightened. The sealing of joints could be done with a gasket named 'Terostat' (impermeable to helium). Due to varying lengths of the rock samples there were two aluminium slabs with different thicknesses (24,4 mm and 28,0 mm).

The nitrogen gas could be conducted from the container in the laboratory via a pressure meter to the flushing side of the sample and the (over)pressure of the nitrogen could be tuned by the adjusters in the nitrogen container. The mixture of helium and nitrogen could be led to the helium sniffer via a choker (could be used to limit the helium flow, but this was not necessary in experiments of this thesis). The helium sniffer worked as

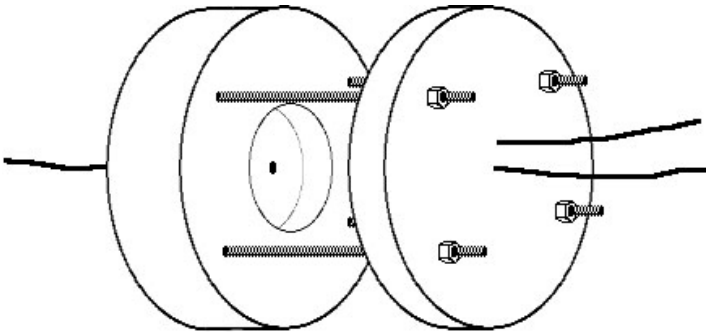

Figure 5.2: *The aluminium discs of the sample holder.*

a mass spectrometer, so it used magnetic and electric fields to select the appropriate isotope of the helium (charge +2e, mass number 4)[1].

The helium gas could be led to the sample holder via a (six-way) selector valve. There were three different positions for the selector valve: position 1 (Inj.) the valve connected the injection chamber of the sample to the one coming from the shut-off valve. In position 2 (Vac.) the injection chamber was connected to the vacuum pump and in position 3 (Perm.) straight to the helium container.

From the shut-off valve (which could be adjusted to close or open the pipe) the pipelines continued to another valve (named injector), with two possible positions. In position 1 (Load.) injector connected the flushing nitrogen to the shut-off valve and in addition it connected the helium container with the (inlet side of the) loop. In addition, the outlet side of the loop was connected to room air). So, in this position the helium gas could flow from the container to the loop and (after filling it) to the room air. In position 2 (Inj. /Perm.) the nitrogen container and the inlet of the loop and also the outlet of the loop and the shut-off valve were connected. The selector valve and the injector could also be held at positions between the above mentioned positions, in which case the pipes were not connected. The structure of the apparatus is presented in figure 5.3.

The two pressure meters measured the relative overpressure compared to the room air, and thus e.g. when speaking of the pressure of the flushing nitrogen to be 1 kPa, an overpressure of 1 kPa is meant.

In addition there was a vacuum oven, where rock samples were kept. Both warming and vacuum ventilation could be turned on, which resulted in removal of water from

[1]The helium sniffer ionized the atoms, which resulted in the above mentioned positive charge [60].

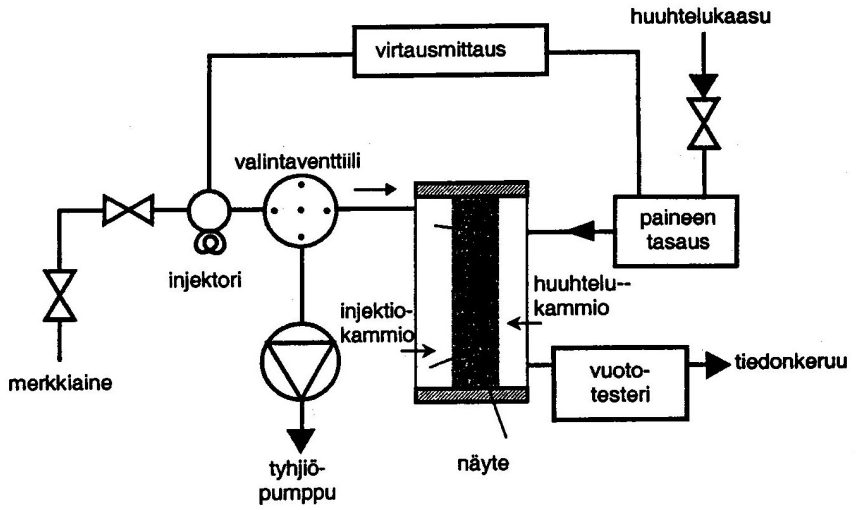

Figure 5.3: *A schematic representation of the apparatus [60].*

the pores of the sample. After the water was removed, nitrogen gas could be led into the oven for preservation of the non-hydration of the samples.

5.2 Methods

Before the actual measurement the rock sample should be sealed leak-proof to the sample holder. This was done by the help of 'Terostat' gasket. There after the pressure meter was connected to the injection side along with the inflow capillary of helium gas. The selector valve was set into position 2 (Vac.) and the pressure was determined. If the vacuum reached a value of -90 kPa quite rapidly, the packing was successful. If there were leaks or other problems in the system, a vacuum of this magnitude was not achieved. A similar checking was executed on the flushing side. If the pressure of the chamber was not satisfactory, the system was dismantled and the sample was sealed again.

The initial amount of helium in the sample (due to previous measurements) was quite irrelevant in the permeability measurements, since the helium flow saturated at a certain value after waiting long enough.

Before the measurements the pressure gauge was connected to the injection side of the

sample. Helium valves were opened and the selector valve was turned to position 2 (Vac.), causing underpressure on the injection side of the sample. When the pressure was e.g. -20 kPa, the selector valve was set to position 3 (Perm.) and helium gas flowed into the injection cell due to the pressure difference. The selector valve was let to remain in this position (3), because it was desirable to maintain the helium pressure constant in the injection cell. When the helium gas of the injection chamber flowed through the sample, it was replaced by new helium from the helium container [60]. The control program was launched, and the pressures on the flushing and injection sides could be monitored in addition to the time-dependent helium flow.

The pressure of the helium chamber was set to an initial value. This initial pressure varied depending on the rock sample. For some samples the pressure of 5 kPa was enough, while the least porous samples needed an initial pressure of about 50 kPa. The pressure range used was chosen such that the measured helium flow saturated at a constant level in a reasonable time. On the other hand, too great pressures were avoided due to the risk of promoting leaks in system. In addition, a high flow rate could result in an inaccurate value for the helium flow. When the pressure was set to a constant value, helium flow through the sample was let to stabilize.

After saturation of the flow the same process was repeated for a higher pressure value. As the value of permeability would finally appear from a linear fit to the helium flow data (each step corresponding to one measurement point), the number of pressure values had to be sufficient.

Experiments showed that it was a good strategy to set the initial pressure to quite a large value (tens of kPa's) and let the helium flow stabilize for many hours (sometimes for over a night). This caused the pores to be filled with helium, and after that the inlet pressure could be increased by smaller steps, such that the helium flow saturated rapidly. Especially for very porous samples, this was a successful method. The helium flow and the injection pressure as a function of time resulting from a measurement of this kind is shown in figure 5.4.

After such a measurement, it was found to be better to repeat the measurement instead of starting a new kind of, e.g. a diffusion, measurement. If the pressure was dropped to a value of about that of the initial pressure of a new permeability measurement, the helium flow decayed rapidly to the saturation value. After that the whole set of measurements for varying pressure values was easy to carry out.

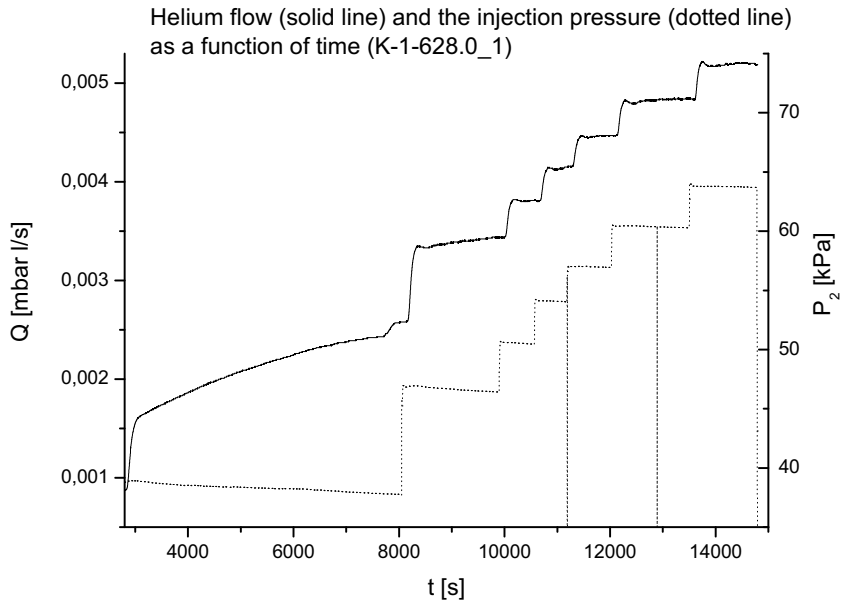

Figure 5.4: *An example of the permeability measurements. The helium flow saturated well after two pressure steps.*

Chapter 6

Observations and calculations

6.1 Method to obtain permeability

To analyze the permeability measurements, the OriginPro 7.5 program (and Microsoft Excel within it) was used. During the measurement the operating system had measured and saved the data of helium flow and pressures on both sides of the sample, as a function of time. The helium sniffer used gave the value of the helium flow in units of mbar l/s. It was assumed that the ambient pressure in the laboratory was 1,013 bar, and that this was also the pressure in the outlet (flushing) chamber. By dividing the measured helium flow by 1,013, it was expressed in units of ml/s. The pressure gauges measured the relative overpressure and thus the absolute pressure was obtained by adding 1,013 bar to the measured values.

During diffusion measurements it was noticed that from the amount of 5 ml helium gas injected into the injection side of the sample, only a portion was detected by the helium sniffer (typically 2 – 4,5 ml). Thus all the helium led to the helium sniffer was not detected, and the measured helium flow had to be calibrated by a calibration factor (the real helium flow was greater than the measured). This calibration factor was estimated by the average helium portion measured during the diffusion measurements of the same sample.

The helium gas used in the measurements was taken from the helium container of the Physics Department (not from a container in the laboratory, as it was the case for nitrogen), and there may have been variations in the quality of the inflowing helium. This would partly explain why the observed helium portions varied in different diffusion

measurements on the same sample. During a permeability measurement helium was continuously added to the injection side, which was assumed to equalize variations in the helium concentration. This is why the average helium portion was used when determining the permeability.

The end of the sample was approximately a circle and thus its area was calculated as $A = \pi r^2$. The length of the sample was taken to be the length (the ends of the sample were not always exactly parallel). In addition, it was known that the viscosity of helium gas was $\mu = 2,0 \cdot 10^{-5} \frac{\text{kg}}{\text{ms}}$ (at 300 K [5]), and helium flow - pressure points were transformed into form of eqn (2.7).

The helium flow and the injection pressure were plotted in the same graph. For each step the region where the helium flow was saturated was estimated visually (in a time frame of hundreads to thousands of seconds). For this region the pressures and the helium flow were averaged. The pressure at the injection was rarely exactly constant in the saturation region, and the use of average values was justified.

The same procedure was repeated for each step of the permeability measurement. A linear fit was made to determine the permeability when the data were expressed in the form of eqn (2.7). All these steps in the determination of permeability are shown in figure 6.1.

The product of specific area and tortuosity were determined for the samples using eqn (2.12). The porosity (measured by Mikko Voutilainen), permeability and above product are shown for all samples in table 6.1.

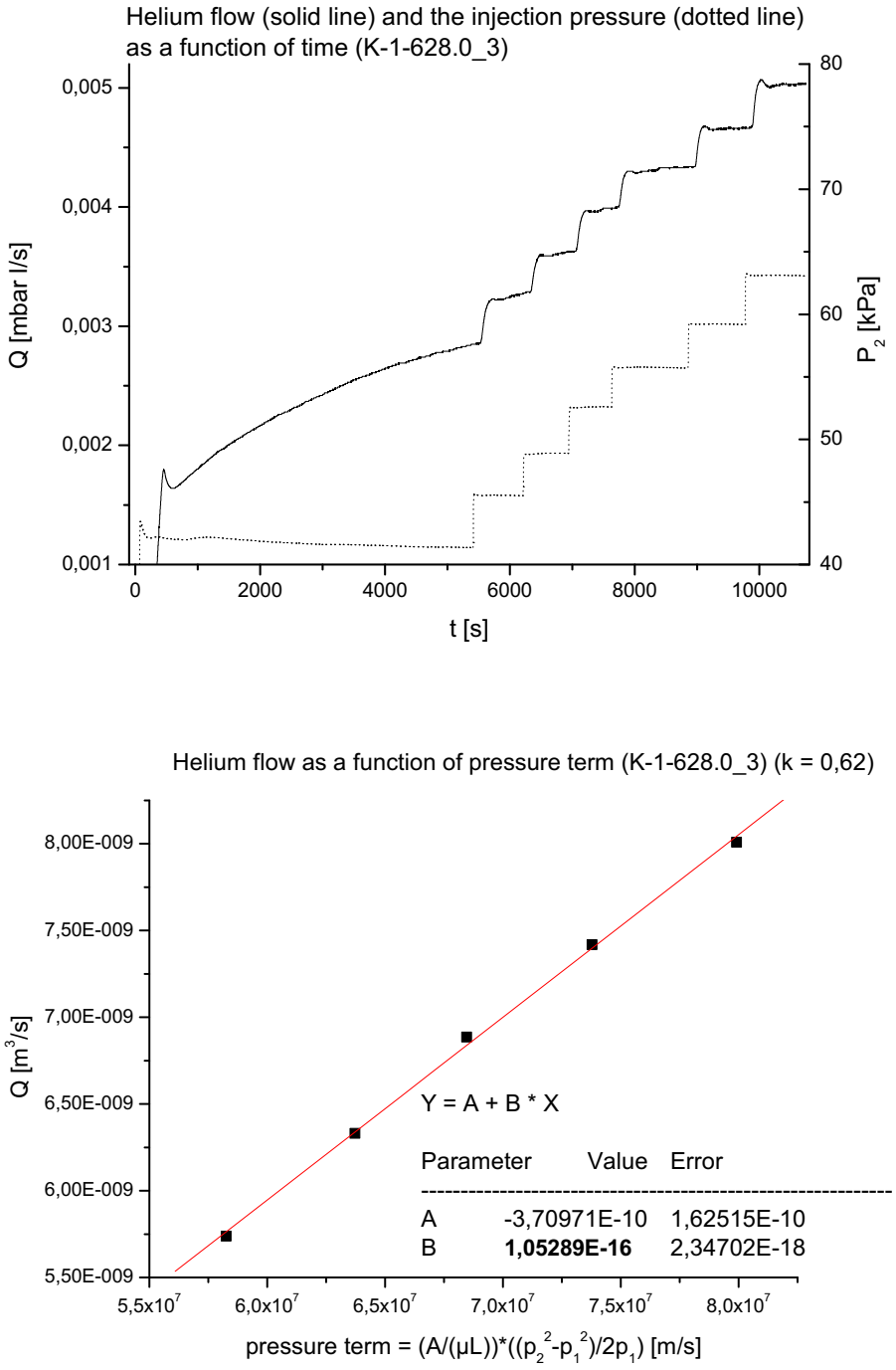

Figure 6.1: *An example of the permeability measurements. In the upper figure helium flow and the corresponding pressure are shown as a function of time. In the lower figure the helium flow is given as a function of the pressure term together with a linear fit to the data.*

Table 6.1: *Porosities, permeabilities and calibration factors of the rock samples*

sample number	porositys ϵ_p[%]	permeability k[m^2]	calibration factor η	$A_0\tau$ [m^2]
415.108.0	0,4	$1{,}0 \cdot 10^{-21}$	0,585	$2{,}5 \cdot 10^{6}$
415.67.0	1,5	$\sim 10^{-20}$	(0,585)	$1{,}0 \cdot 10^{6}$
K-18-430.7	3,3	$1,6 \pm 0,2 \cdot 10^{-17}$	0,552	$3{,}1 \cdot 10^{6}$
K-1-782.4	4,6	$1,40 \pm 0,15 \cdot 10^{-16}$	0,445	$2{,}8 \cdot 10^{5}$
K-1-489.1	8,5	$6,9 \pm 1,0 \cdot 10^{-17}$	0,593	$9{,}0 \cdot 10^{6}$
K-12-449.0	10,8	$2,0 \pm 0,2 \cdot 10^{-18}$	0,70	$4{,}9 \cdot 10^{5}$
K-1-556.0	15,6	$5,4 \pm 0,6 \cdot 10^{-17}$	0,635	$1{,}2 \cdot 10^{7}$
K-18-391.7	11,8	$4,0 \pm 0,4 \cdot 10^{-17}$	0,47	$4{,}6 \cdot 10^{6}$
K-12-458.2	20,1	$3,2 \pm 0,4 \cdot 10^{-17}$	0,47	$1{,}3 \cdot 10^{7}$
415.76.0	16,8	$5,8 \pm 0,6 \cdot 10^{-18}$	0,56	$2{,}2 \cdot 10^{7}$
K-1-475.3	5,5	$5,9 \pm 0,7 \cdot 10^{-18}$	0,27	$3{,}6 \cdot 10^{6}$
415.191.0	0,9	$4,0 \pm 0,5 \cdot 10^{-21}$	(average)	$2{,}7 \cdot 10^{6}$
K-1-628.0	2,5	$1,06 \pm 0,11 \cdot 10^{-16}$	0,62	$2{,}5 \cdot 10^{5}$
K-1-400.5	11,9	$2,9 \pm 0,3 \cdot 10^{-18}$	0,61	$5{,}5 \cdot 10^{6}$
K-1-740.8	5,1	$2,9 \pm 0,3 \cdot 10^{-17}$	0,53	$1{,}4 \cdot 10^{6}$
K-12-395.7	10,2	$8,5 \pm 0,9 \cdot 10^{-17}$	0,74	$2{,}5 \cdot 10^{6}$
K-12-441.8	6,4	$1,21 \pm 0,13 \cdot 10^{-15}$	0,60	$3{,}1 \cdot 10^{5}$
K-1-503.2	13,6	$3,1 \pm 0,4 \cdot 10^{-17}$	0,71	$6{,}6 \cdot 10^{6}$
K-1-534.7	11,1	$7,9 \pm 0,9 \cdot 10^{-16}$	0,68	$9{,}4 \cdot 10^{5}$
K-18-380.2	26,6	$8,9 \pm 0,9 \cdot 10^{-16}$	0,062	$4{,}0 \cdot 10^{6}$
K-1-476.5	0,4	$9,7 \pm \cdot 10^{-19}$	0,088	$1{,}6 \cdot 10^{5}$

6.2 Results

In addition to permeabilities, the diffusion coefficients D_e of the rock samples were measured. The theoretical backround and a description of diffusion measurement process will be explained elsewhere, but we show the results here in order to draw conclusions on the relationships between structural and transport parameters.

The permeability of the rock samples is shown versus their porosity in figure 6.2. Points in this graph can be divided into two groups. In the lower left corner of the plot there is a group of four points, and the rest 17 points form another group in the upper right corner of the plot. Within these groups there is no correlation, but as a whole there is a tendency that permeability increases with increasing porosity, which is to be expected.

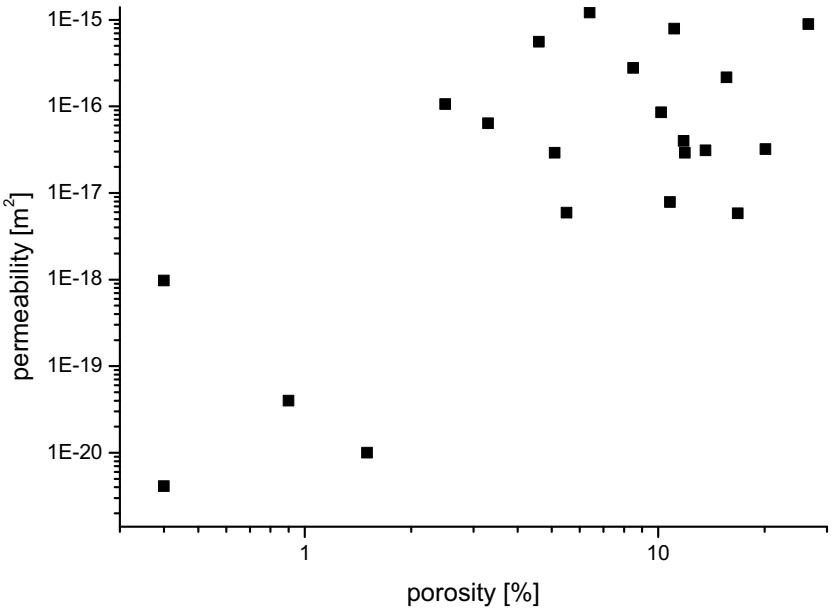

Figure 6.2: *Permeability as a function of porosity.*

These two groups are also present in the plot of tortuosity times specific area (denoted as $\chi := A_0 \cdot \tau$) against porosity, figure 6.3. This quantity, χ, increases with increasing porosity within each group separately. This behaviour counteracts the effect of porosity on permeability. However, the variation of χ is only about two orders of magnitude, and this quantity cannot explain the lowest permeabilities observed in the samples. There is no overall correlation between the χ parameter and porosity.

It is evident from figure 6.4 that diffusion coefficient and permeability have a fairly close

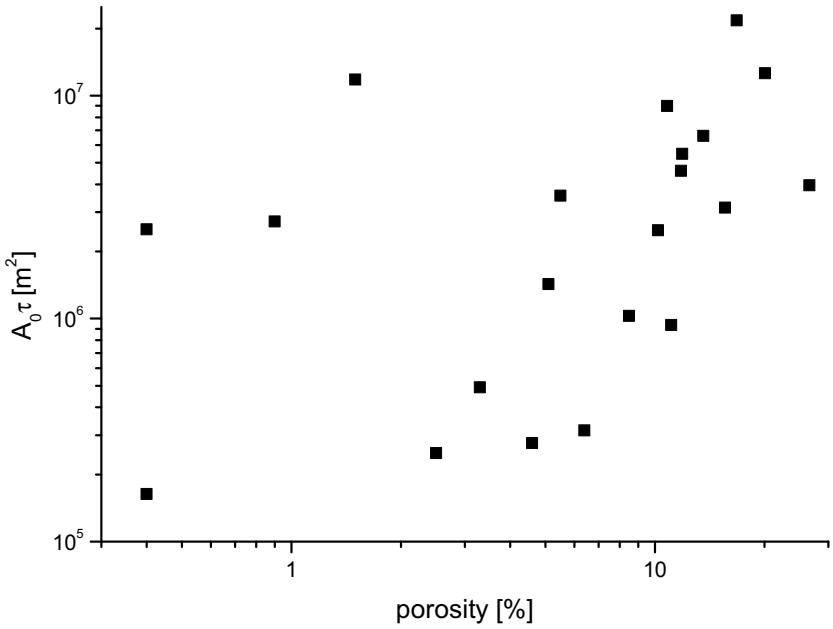

Figure 6.3: *The product of tortuosity τ and specific area A_0 as a function of porosity.*

correlation. As permeability increases, so does the diffusion coefficient. Both quantities characterize the amount of flow through the sample. If we fit a linear regression to this graph, its slope equals 0,37, and there is thus a relationship $D_e \propto k^{0,37}$ between the two quantities.

The permeability and porosity were also plotted as a function of depth from which the sample was taken. Permeability showed a minor positive correlation with depth, whereas porosity did not correlate appreciably. It can also be concluded that rock samples from a depth range of 400 – 550 m had relatively high permeability and porosity.

The product of tortuosity and specific area did not seem to depend on the depth. The rock samples from shallow depths (0 – 200 m) seemed to have a high value of χ, but as there were only four measurement points in that region, this observation does not have statistical significance.

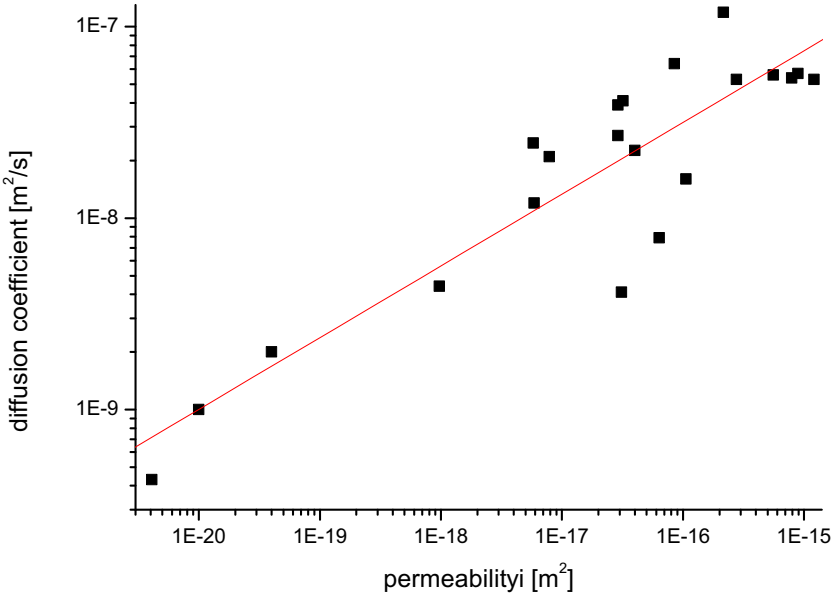

Figure 6.4: *Diffusion coefficient as a function of permeability and a linear fit.*

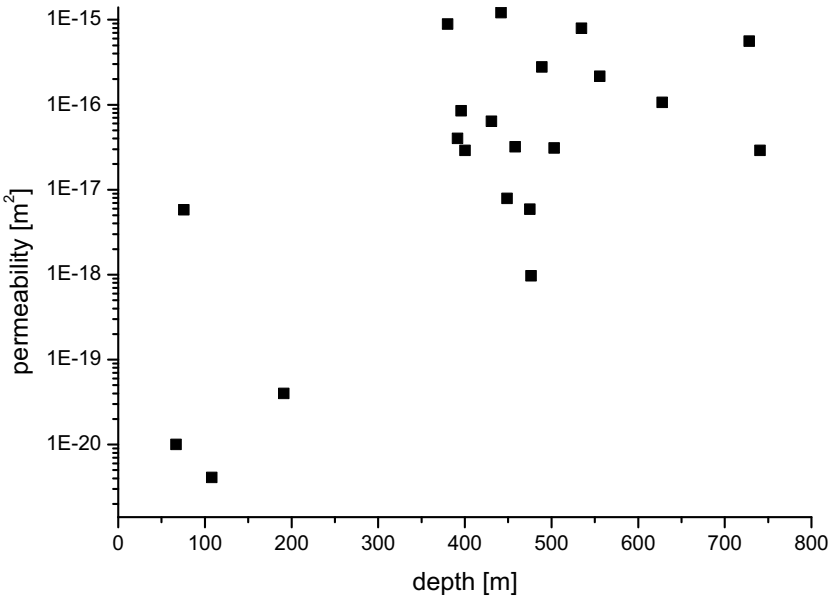

Figure 6.5: *Permeability as a function of depth.*

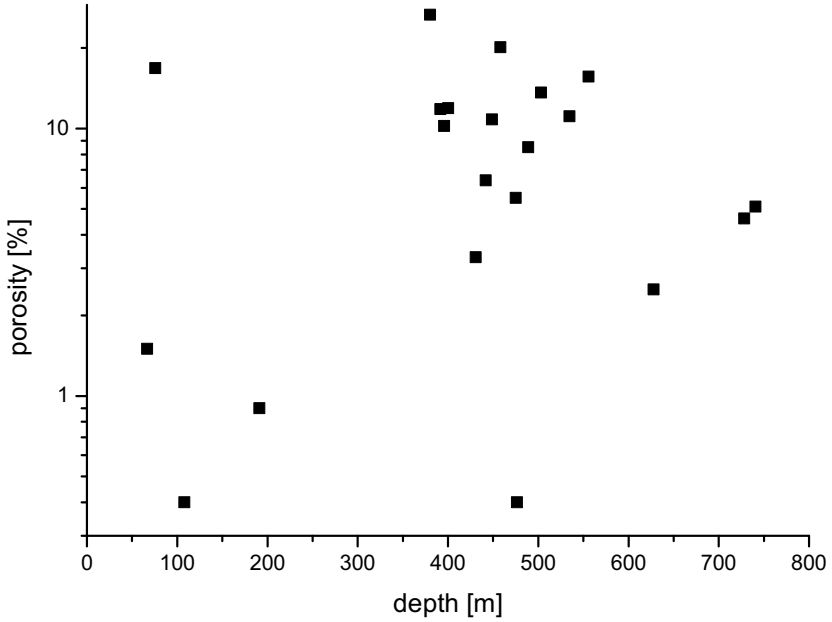

Figure 6.6: *Porosity as a function of depth.*

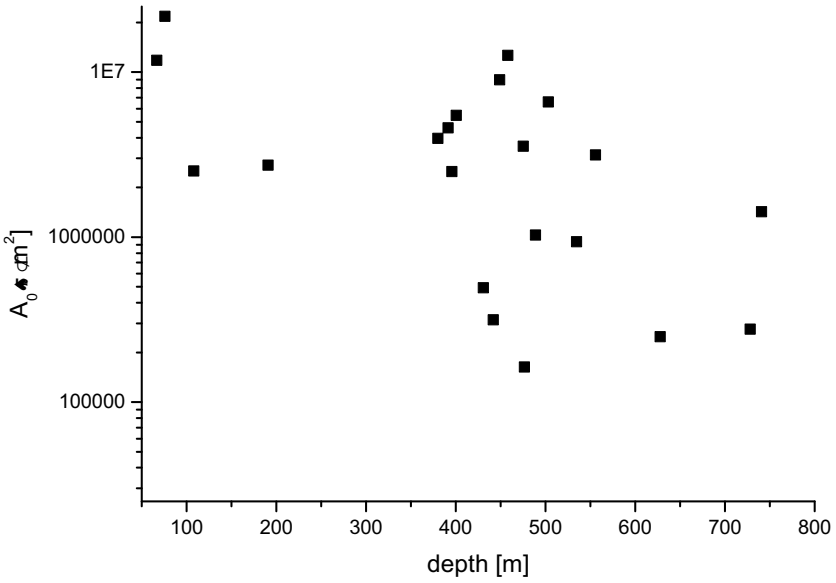

Figure 6.7: *The product of tortuosity τ and specific area A_0 as a function of depth.*

6.3 Encountered problems

Sometimes the pressure gauge at the injection side indicated zero pressure, which could be seen as a vertical line in the pressure graph. Taking averages eliminated this error source.

Occasionally the first helium flow values corresponding to the first pressure steps were not well saturated, and they were excluded from the permeability determination (linear fit). Helium flow at high pressure values (especially in samples of high porosity) could be so high ($\sim 10^{-2}$ ml/s) that the helium sniffer no longer measured it reliably, and these values were also excluded from the permeability determination.

Sometimes the helium flow increased unnaturally rapidly, which propably indicated movement of gasket, resulting in a helium leak past the sample. This caused the injection pressure and thus the helium flow to drop. This phenomenon was typically observed at high injection pressures. Such an event was observed in sample K-1-475.3, and it is shown in figure 6.8. Sometimes this problem was solved simply by using smaller pressures, but sometimes the only solution was to open the package and to seal it again.

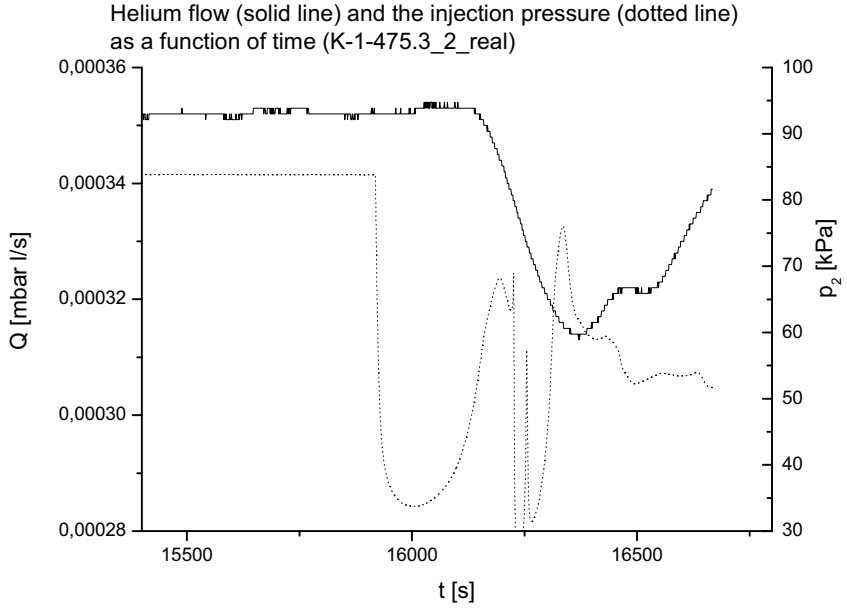

Figure 6.8: *An example of failing of gasket. The pressure suddenly drops and starts to behave arbitrarily.*

At times a leak was observed in a less dramatic way: the pressure in the injection chamber was not constant, but decreased in a gradual yet noticeable way. This kind of steps were as well excluded from the permeability determination - the package had to be sealed again.

For an unknown reason, at times the helium flow started to oscillate. Sometimes the oscillation was so remarkable, that the measurement had to be stopped and the package resealed. Sealing solved the problem and thus it was a problem in the packing, not in the sample. Such an oscillation is shown in figure 6.9.

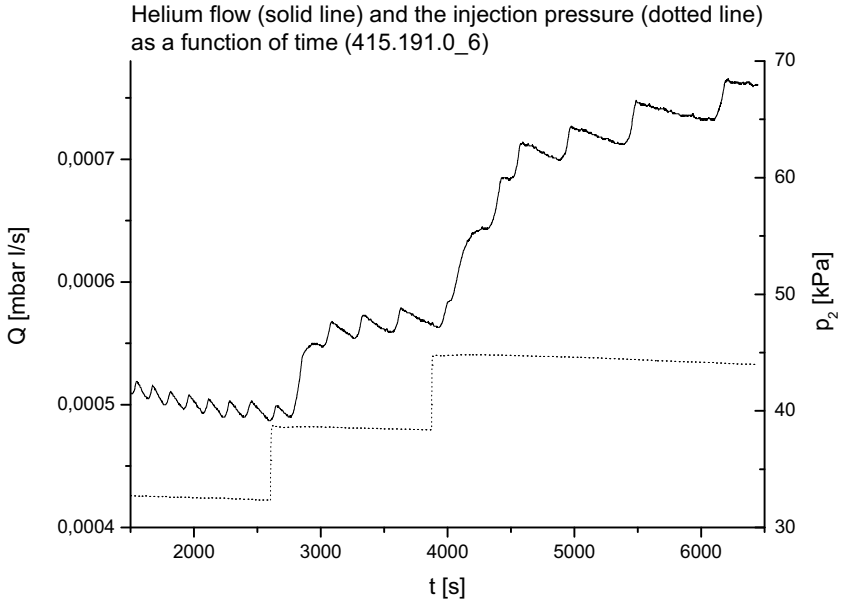

Figure 6.9: *An example of oscillatory behaviour.*

Some rock samples were found to have a major macroscopic flow channel through them. Whenever applying a pressure on one side of the sample, the pressure on the other side of the sample started to saturate at about the same level (this was observed during vacuum tests). When setting a certain pressure on the injection side, the flow reached quite a high value. After that a rise in the injection pressure had no effect on the helium flow (shown in figure 6.10) - all the helium flowed rapidly through the sample regardless of the pressure. For these rock samples, the permeability was impossible to determine.

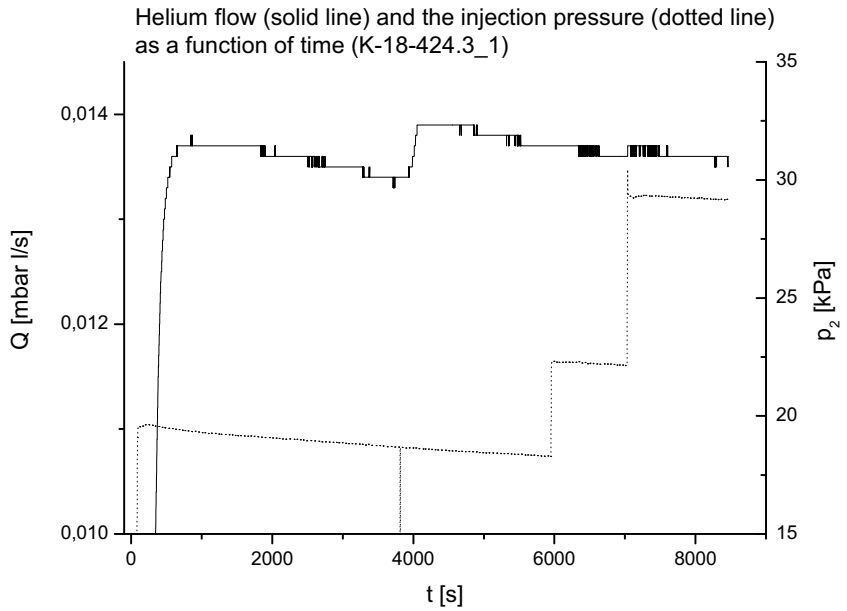

Figure 6.10: *An example of permeability measurement of a rock sample which is likely to have a major flow channel (fracture) through it.*

Chapter 7

Conclusions

Geothermal energy is a clean and renewable source of energy, which can contribute to world's energy production significantly due to its high energy potential. The Hot Dry Rock method in geothermal energy utilization is a very promising method as it has the potential to produce significant amounts of renewable, sustainable and clean energy for almost everywhere in the world, throughout the year. Another advantage of HDR energy is its flexibility, which allows adjusting the production to meet the electrical load.

Warming up of the circulating water occurs several kilometres under the surface of the Earth, which is sure to generate vast technical problems, including drilling techniques, relative uncontrollability of hydraulic fracturing and water losses. Also the natural circumstances in a HDR reservoir (high temperature and pressure) pose challenging engineering problems. Accurate information about the reservoir is crucial in order to simulate processes taking place even adequately. Having reasonable measurement systems is a key question for developing HDR technology. Also the need for mathematical modelling and optimization of the HDR method is evident, but due to the complex nature and non-linear behaviour of an HDR reservoir, it must be done with care.

Thus, the HDR method suffers from vast problems and it is still more at a state of scientific and experimental research than at a state of actual exploitation. However, the results obtained by pilot HDR projects around the world sound promising, and this unique energy technology is about to reach an economically viable level.

One of the most vital parameters of an HDR plant is the permeability of the reservoir. Much effort in the development of the HDR method is concentrated on the estimation of

permeability and on finding ways to increase it. The permeability measuring equipment at the University of Jyväskylä is of good standard and as an example the permeabilities of 21 rock samples from Kaali meteor crater were measured.

Leaving out the least porous samples, determination of permeability was successful. Despite the fact that helium flow did not always saturate perfectly, averaging of results produced quite reliable values for permeability (the error in the slope of a linear fit was reasonably small). Also, in the light of fundamental difficulties related to permeability measurements, the differences between measurements on the same sample were acceptably small. The product of specific surface area and tortuosity, χ, was calculated based on the Carman-Kozeny expression using measured values of permeability and porosity. Because the errors in the porosities were relatively small [1], the reliability of χ resembled that of permeability.

The greatest source of error in permeability measurements was the calibration factor. The observed helium portion varied significantly between diffusion measurements of one rock sample. Although the calibration factor was calculated as an average of observed amounts of helium, there were typically only three such measurements, and thus a significant error remained in the value of the calibration factor.

In order to mitigate this error source, a precise analysis considering why the helium sniffer did not observe all the helium should be carried out. Also, the dependence of the calibration factor on the amount of helium flow should be investigated, because the helium flows were naturally low in the diffusion measurements (in the absence of pressure gradient).

No exact literature values were available for the permeabilities (or for the values of χ) of these rock samples, but the results were of a reasonable magnitude [2].

Bibliography

[1] Voutilainen, M., *Kaalin kraatterin kivinäytteiden huokoisuuden ja kokonaistilavuuden määrittäminen*, Master's thesis, University of Jyväskylä, Department of Physics, 2005.

[2] Nield, A. and Bejan, A., *Convection in porous media*, 2nd edition, Springer-Verlag, New York, NY, 1999.

[3] Johnson, R. (ed.), *The handbook of fluid dynamics*, CRC Press, Boca Raton, FL, 1998.

[4] Dullien, F., "Porous media: fluid transport and pore structure", Academic Press, San Diego, 1979.

[5] Lide, D., *et. al.*, "CRC Handbook of Chemistry and Physics", 74th edition, CRC Press, Boca Raton, FL, 1993.

[6] Freedman, R., and Young, H., *University physics with modern physics*, Addison-Wesley, 11th edition, San Francisco, Ca, 2004.

[7] White, F., *Fluid Mechanics*, 5th edition, McGraw-Hill, New York, NY, 2003.

[8] Godfrey Boyle (editor), "Renewable energy: power for a sustainable future", Oxford University Press, New York, 2004.

[9] Dickson, H. and Fanelli, M. (editors), "Geothermal energy: utilization and technology", United Nations Educational, Scientific and Cultural Organisation, Paris, 2003.

[10] Barbier, E., *Geothermal energy technology and current status: an overview*, Renewable and Sustainable Energy Reviews **6** (2002) 3-65.

[11] Incropera, F. and Dewitt, D., "Fundamentals of heat and mass transfer", John Wiley & Sons, 5th edition, New York, NY, 2002.

[12] Abé, H., Duchane, D., Parker, R., and Kuriyagawa, M., *Present status and remaining problems of HDR/HWR system design*, Geothermics **28** (1999) 573-590.

[13] Fridleifsson, I., *Status of geothermal energy amongst the world's energy sources*, Geothermics **32** (2003) 379-388.

[14] International Geothermal Association IGA, *Geothermals in the world*, retrieved 28.6.2007 from `http://iga.igg.cnr.it/geoworld/geoworld.php?sub=duses`.

[15] Lund, J., Freeston, D., and Boyd, T., *Direct application of geothermal energy: 2005 Worldwide review*, Geothermics **34** (2005) 690-727.

[16] Kukkonen, I., *Geothermal energy in Finland*, Proceedings, World Geothermal Congress, Kyushu-Tohoku, Japan, 2000.

[17] *Geothermal energy development in Europe - an insight into current methods and trends*, Orkustofnun, the National Energy Authority of Iceland, retrieved 16.11.2006 from `http://www.os.is/Apps/WebObjects/Orkustofnun.woa/swdocument/2043/`.

[18] Stefansson, V. and Axelsson, G., *Sustainable benefits of geothermal utilization*, International Geothermal Workshop, Sochi, Russia, 2003.

[19] Sanyal, S., *Sustainability and renewability of geothermal power capacity*, Proceedings, World Geothermal Congress, Antalya, Turkey, 2005.

[20] Rybach, L., *Geothermal energy: sustainability and the environment*, Geothermics **32** (2003) 463-470.

[21] Kristmannsdóttir, H., Ármannsson, H., *Environmental aspects of geothermal energy utilization*, Geothermics **32** (2003) 451-461.

[22] Brophy, P., *Environmental advantages to the utilization of geothermal energy*, Renewable Energy **10** (1997) 367-377.

[23] El-Wakil, M., "Powerplant Technology", McGraw-Hill, Ohio, 1984.

[24] European deep geothermal energy programme. Retrieved 20.6.2007 from `http://www.soultz.net/version-en.htm`.

[25] Baria, R., Baumgärtner, J., Rummel, F., Pine, R., and Sato, Y., *HDR/HWR reservoirs: concepts, understanding and creation*, Geothermics **28** (1999) 533-552.

[26] Nakatsuka, K., *Field characterization for HDR/HWR: a review*, Geothermics **28** (1999) 519-531.

[27] Evans, K., Cornet, F., Hashida, T., Hayashi, K., Ito, T., Matsuki, K., and Wallroth, T., *Stress and rock mechanics issues of relevance to HDR/HWR engineered geothermal systems: review of developments during the past 15 years*, Geothermics **28** (1999) 455-474.

[28] Tran, N. and Rahman, S., *Development of hot dry rocks by hydraulic stimulation: Natural fracture network simulation*, Theoretical and Applied Fracture Mechanics **47** (2007) 77-85.

[29] Butler, S., Sanyal, S., and Robertson-Tait, A., *A numerical simulation study of the performance of enhanced geothermal systems*, Proceedings, 29th Workshop on Geothermal Reservoir Engineering, Stanford University, Palo Alto, Ca, 2004.

[30] Sasaki, S. and Kaieda, H., *Determation of stress state from focal mechanisms of microseismic events induced during hydraulic injection at the Hijori hot dry rock site*, Pure and applied geophysics **159** (2002) 489-516.

[31] Parker, H. and Jupe, A., *In situ leach mining and hot dry rock (HDR) geothermal energy technology*, Minerals Engineering **10** (1997) 301-308.

[32] Wallroth, T., Jupe, J., and Jones, H., *Characterisation of a fractured reservoir using microearthquakes induced by hydraulic injections*, Marine and Petroleum Geology **13** (1996) 447-455.

[33] Mégel, T., Kohl, T., and Hopkirk, R., *The potential of the use of dense fluids for initiating hydraulic stimulation*, Geothermics **35** (2006) 589-599.

[34] Baisch, S., Weidler, R., Voeroes, R., Tenzer, H., Teza, D., *Improving hydraulic stimulation efficiency by means of real-time monitoring*, 29th Workshop on Geothermal Reservoir Engineering, Stanford University, Palo Alto, Ca, 2004.

[35] Oilfield Glossary. Retrieved 25.10.2006 from `http://www.glossary.oilfield.slb.com/Display.cfm?Term=proppant`.

[36] Murphy, H., Brown, D., Jung, R., Matsunaga, I., and Parker, R., *Hydraulics and well testing of engineered geothermal reservoirs*, Geothermics **28** (1999) 491-506.

[37] Brown, D., DuTeaux, R., Kruger, P., Swenson, D., and Yamaguchi, T., *Fluid circulation and heat extraction from engineered geothermal reservoirs*, Geothermics **28** (1999) 553-572.

[38] Mégel, T., Kohl, T., Gérard, A., Rybach L., and Hopkirk R., *Downhole pressures derived from wellhead measurements during hydraulic experiments*, Proceedings, World Geothermal Congress, Antalya, Turkey, 2005.

[39] Baujard, C., Bruel, D., *Numerical study of the impact of fluid density of the pressure distribution and stimulated volume in the Soultz HDR reservoir*, Geothermics **35** (2006) 607-621.

[40] Grecksch, G., Jung, R., Tischner, T., and Weidler, R., *Hydraulic fracturing at the European HDR/HFR test site Soultz-sous-Forêts (France) - a conceptual model*, European Geothermal Conference, Szeged, Hungary, 2003.

[41] Kohl, T., Mégel, T., Baria, R., Hopkirk, R., and Rybach, L.,, *Determining the impact of massive hydraulic stimulation of local microseismicity*, Proceedings, World Geothermal Congress, Antalya, Turkey, 2005.

[42] Editorial, *The deep EGS (Enhanced Geothermal System) project at Soultz-sous-Forêts (Alsace, France)*, Geothermics **35** (2006) 473-483.

[43] Baumgärtner, J., Teza, D., Hettkamp, T., Homeier, G., Baria, R., and Michelet, S., *Electricity production from hot rocks*, Proceedings, World Geothermal Congress, Antalya, Turkey, 2005.

[44] Abé, H., Niitsuma, H., Murphy, H., *Summary of discussions, structured academic review of HDR/HWR reservoirs*, Geothermics **28** (1999) 671-679.

[45] Niitsuma, H., Fehler, M., Jones, R., Wilson, S., Albright, J., Green, A., Baria, R., Hayashi, K., Kaieda, H., Tezuka, K., Jupe, A., Wallroth, T., Corneth, F., Asanuma, H., Moriya, H., Nagano, K., Phillips, W., Rutledge, J., House, L., Beauce, A., Alde, D., and Aster, R., *Current status of seismic and borehole measurements for HDR/HWR development*, Geothermics **28** (1999) 475-490.

[46] Sanjuan, B., Pinault, J., Rose, P., Gérard, A., Brach, M., Braibant, G., Crouzet, C., Foucher, J., Gautier, A., and Touzelet, S., *Tracer testing of geothermal heat exchanger at Soultz-sous-Forêts (France) between 2000 and 2005*, Geothermics **35** (2006) 622-653.

[47] Hayashi, K., Willis-Richards, J., Hopkirk, R., and Niibori, Y., *Numerical models of HDR geothermal reservoirs - a review of current thinking and progress*, Geothermics **28** (1999) 507-518.

[48] Jupe, A., Bruel, D., Hicks, T., Hopkirk, R., Kappelmeyer, O., Kohl, T., Kolditz, O., Rodrigues, N., Smolka, K., Willis-Richards, J., Wallroth, T., and Xu, S., *Modelling of a European prototype HDR reservoir*, Geothermics **24** (1995) 403-419.

[49] O'Sullivan, M., Pruess, K., and Lippmann, M., *State of art of geothermal reservoir simulation*, Geothermics **30** (2001) 395-429.

[50] Vörös, R., Wiedler, R., de Graaf, L., Wyborn, D., *Thermal modelling of long term circulation of multi-well development at the Cooper Basin hot fractured rock (HFR) project and current proposed scale-up program*, Proceedings, 32th Worshop on Geothermal Reservoir Engineering, Stanford, Palo Alto, Ca, 2007.

[51] Duchane, D., *Geothermal energy from hot dry rock: A renewable energy technology moving towards practical implementation*, Earth and environmental sciences division, Los Alamos, New Mexico, 1996.

[52] Kaya, T. and Mertoglu, O., *Engineering aspects of geothermal production well with down hole pumps*, Proceedings, World Geothermal Congress, Antalya, Turkey, 2005.

[53] Ghassemi, A. and Tarasovs, S., *Three-dimensional modeling of injection induced thermal stresses with an example from Coso*, Proceedings, 29th Workshop on Geothermal Reservoir Engineering, Stanford University, Palo Alto, Ca, 2004.

[54] Ghassemi, A. and Kumar, G., *Changes in fracture aperture and fluid pressure due to thermal stress and silica dissolution/precipitation induced by heat extraction from subsurface rocks*, Geothermics **36** (2007) 115-140.

[55] Ghassemi, A. and Zhang, Q., *Poro-thermoelastic mechanisms in wellbore stability and reservoir stimulation*, Proceedings, 29th Workshop on Geothermal Reservoir Engineering, Stanford University, Palo Alto, Ca, 2004.

[56] Ghassemi, A. *Stress and pore pressure distribution around a pressurized, cooled crack in low permeability rock*, Proceedings, 32th Workshop on Geothermal Reservoir Engineering, Stanford University, Palo Alto, Ca, 2007.

[57] André, L., Rabemanana, V., and Vuataz, F., *Influence of water-rock interactions of fracture permeability of the deep reservoir at Soultz-sous-Forêts, France*, Geothermics **35** (2006) 507-531.

[58] Jing, Z., Watanabe, K., Willis-Richards, J., and Hashida, T., *A 3-D water/rock chemical interaction model for prediction of HDR/HWR geothermal reservoir performance*, Geothermics **31** (2002) 1-28.

[59] Rabemanana, V., Vuataz, F., Kohl, T., and André, L., *Simulation of mineral precipitation and dissolution in the 5-km deep enhanced geothermal reservoir at Soultz-sous-Forêts, France*, Proceedings, World Geothermal Congress, Antalya, Turkey, 2005.

[60] Maaranen, J., *Kiinteän aineen efektiivisen diffuusiokertoimen ja permeabiliteetin määrittäminen heliumkaasumittalaitteistolla*, Master's thesis, University of Jyväskylä, Department of Physics, 2000.

[61] Taylor, J., *An introduction to error analysis: the study of uncertainties in physical measurements*, University Science Books, Sausalito, Ca, 1997.

Appendix A

Error estimation

Permeability measurements were independent measurements with a varying uncertainty and thus the weighted average [61] was used to estimate the statistical error of these measurements. We denote the values of mutually independent measurements by x_i and their uncertainties by δx_i. The statistical error in the slope of linear fit was considered to be the error in that particular permeability measurement.

The weighted average and its error of such a set of measurements is given by

$$x = \frac{\sum_{i=1}^{N} \frac{1}{\delta x_i^2} x_i}{\sum_{i=1}^{N} \frac{1}{\delta x_i^2}} \tag{A.1}$$

$$\delta x = \frac{1}{\sqrt{\sum_{i=1}^{N} \frac{1}{\delta x_i^2}}} \tag{A.2}$$

The statistical error from eqn (A.2) was not sufficient to properly describe the uncertainties in the determined value of permeability. There were numerous sources of systematical error, among which the calibration factor was probably the greatest.

It would have been possible to estimate the error of each "permeability step", for example by the law of quadratic propagation of the error. The error estimated in this way was of the order of 10 %. Typically the Terostat gasket covered some millimeters

of the end of the sample, causing an error in the cross-section area A. There was also an error related to the length of the sample, because the ends of the sample were not always parallel. Also the viscosity of helium was obtained at a temperature of 300 K, probably resulting in a slight error. These errors were typically independent of the number of the measurement and thus could not be seen as a statistical error.[1]

The greatest source of error was probably the calibration factor. The helium portion observed during diffusion measurements varied significantly from a measurement to another. This calibration factor was obtained as an average of a few such measurements (typically 3), and it thus remained quite sensitive to errors. To mitigate this error, one would need to analyze the calibration of the helium sniffer and its dependence on the amount of helium flow. This would mean a rearrengement of the measurement system, and a reliable flow meter at the injection side, which would take into account the compressibility of helium. Secondly, in diffusion helium flows were naturally much smaller than in the permeability measurements, and thus calibration factor obtained from the diffusion measurements may have included a related error.

Thus, in addition to the statistical error, an error of 10 % was estimated to be associated with the measurement process, and this was combined quadratically with the statistical error.

Results were rounded according to the "rule of 15 units". The final results are shown in table 6.1.

[1]Because the package was often sealed only once, after which all the measurements were carried out, the error in the cross-sectional area was also independent of the number of measurement.